PHYSICAL REVIEW B VOLUME 20, NUMBER 10 15 NOVEMBER 1979

# Magnetoluminescence of the electron-hole liquid in germanium

H. L. Störmer*
*Max-Planck-Institut für Festkörperforschung, Hochfeld-Magnet Labor Grenoble, Boîte Postale 166, Centre de Tri, 38042 Grenoble, France*

R. W. Martin†
*Physikalisches Institut der Universität Stuttgart, 7 Stuttgart 80, Pfaffenwaldring 57, Federal Republic of Germany*
(Received 2 April 1979)

We report photoluminescence measurements on the electron-hole liquid (EHL) in germanium in magnetic fields up to 19 T (190 kG). The line shape of the luminescence spectra for allowed (LA) as well as forbidden (TA) transitions could be fitted theoretically taking into account the detailed structure of the conduction and valence bands in a magnetic field. All details of the experimental line shape, including their polarization properties, are well reproduced by their theoretical counterparts over the entire field range. The low-energy tail of the EHL spectra could be described quantitatively by an energy-dependent quasiparticle lifetime. This line-shape analysis yielded the field dependence of the important parameters of the condensed state: equilibrium density, ground-state energy, and work function. It was found that there exists an enhancement of the carrier masses of about 10%. The sum of the exchange and correlation part of the ground-state energy turned out to be only weakly field dependent. Therefore a simple model is proposed which allows the calculation of the field dependence of the basic EHL parameters in an approximate way. The relative intensities of the TA- and LA-phonon replicas are quantitatively described over a large region of magnetic-field strength which confirms earlier findings on the nature of the electron-phonon matrix elements involved. No evidence for a field-induced transition from electron-hole droplets to electron-hole fibers, as predicted theoretically, has been found in our high-field optical experiments.

## I. INTRODUCTION

The electron-hole liquid (EHL) in semiconductors is a discovery of the last decade.[1] At liquid-helium temperatures a high-density gas of nonequilibrium carriers undergoes a phase transition to form a quasistationary two-component Fermi liquid. Electrons and holes populate the lowest-energy states of conduction and valence bands up to Fermi levels $E_F^e$ and $E_F^h$, respectively, uniquely determined by the equilibrium density of the electron-hole liquid and the band parameters. Although this phenomenon has been found in a great variety of semiconductors, Ge has proved to act as a model substance for the thorough study of the properties of the condensate.

In a magnetic field such a degenerate system should show quantum oscillations periodic in $1/H$ in analogy to the well-known de Haas–van Alphen effect in metals. Indeed various kinds of magneto-oscillatory effects have been found, namely magneto oscillations of

(1) the intensity of the $e$-$h$ radiative recombination,[2-7]
(2) the far-infrared absorption,[4,8-11]
(3) the $e$-$h$ lifetime,[6,12] and
(4) the half-width of the luminescence band.[13]

However, the interpretation of these oscillations cannot be as straightforward as in the case of a metal. The simple geometrical constructions, commonly used to interpret magneto oscillations in metals, rely heavily on the fact that the Fermi energy $E_F$ of the electron liquid is much bigger than the energy of the magnetic perturbation, $\hbar\omega_c$, and the thermal energy $kT$. For the EHL in Ge, having Fermi energies of only several meV, both conditions are no longer guaranteed *per se*. In addition a more fundamental difference between the electron liquid in a metal and the electron-hole liquid in a semiconductor enters: In contrast to the case of a metal, the $e$-$h$ density of the liquid is not independent of external perturbations, but adjusts itself to a value that optimizes the total energy of the system, balancing between the repulsive kinetic energy of the particles and their attractive exchange and correlation interaction. All three contributions to the ground-state energy must be considered to be magnetic-field dependent, leading to an explicit field dependence of the density. Nevertheless, magneto-oscillatory effects in the EHL so far have been interpreted in close analogy to the de Haas–van Alphen effect. To justify this approach, an independent data source for the field dependence of the density is highly desirable.

Actually little information concerning the field dependence of the density and related phenomena can be gotten from magneto-oscillatory effects inasmuch as the oscillations cease right at the beginning of the most interesting field range, the quantum limit. This lack of information is unfortunate, for theoretical models predict dramatic effects for the high-field region. The liquid might undergo an additional phase transition to form a hexagonal lattice of $e$-$h$ columns centered around the field lines.[14,15] Again, a detailed study of the field dependence of the ground-state parameters of the condensate, such as the $e$-$h$ density and the ground-state energy, can give indications for the existence of such a phase transition.

In the absence of a magnetic field the method of analyzing the spectral distribution of the radiative $e$-$h$ recombination, the luminescence line shape, has been proven to be a powerful tool to extract the parameters of the EHL.[1] Basically the method is to fit the line shape with a convolution of the well-known (zero-field) densities of states and Fermi functions of electrons and holes with the ground-state parameters considered as free variables. From the spectral position (chemical potential) of the line the ground-state energy and work function are easily determined; the width of the (fitted) line represents the sum of the electron and hole Fermi energies, which immediately translates into an $e$-$h$ density, assuming that the masses of the carriers in the EHL are known.

Being so successful in the absence of a magnetic field, this method should yield reliable data in the presence of a magnetic field, too. However, immediately a serious complication arises. The analysis of the EHL line shape requires a detailed knowledge of the density of states around the extrema of the bands under the influence of a magnetic field. In Ge, the quantization of the electrons into Landau levels is readily accomplished. The fourfold degenerate top of the valence band, however, exhibits a very complicated Landau structure that can only be treated using tedious numerical methods. The calculation of the dispersion of the holes (with respect to $k_H$, the wave vector along the magnetic field) has not been performed until recently.[16,17] This might be the reason that, though magnetoluminescence of EHL was reported earlier, the description and analysis remained qualitative.[18-23]

To obtain a clear picture of the behavior of the EHL under the influence of a magnetic field we therefore studied the magnetoluminescence of Ge at low temperatures. The field range employed extends far beyond previous studies to magnetic fields of up to 19 T (190 kG). We studied intensively the strong polarization effect of the EHL radiation. The experimental procedure is briefly described in Sec. II.

Section III, the central part of this paper, contains a detailed description of the line-shape analysis of the dominant EHL (LA) recombination line in all four polarizations. It is subdivided into several parts. Part III A summarizes briefly the analysis as it is performed in the absence of a magnetic field, introduces nomenclature, and serves as a reference for the line-shape analysis in the presence of magnetic field given in part III B. There the important conduction- and valence-band densities of states are developed and the influence of a quasiparticle liketime on the EHL line shape, reported earlier for the zero-field case, is discussed. Section III C presents the actual numerical calculations. A set of examples demonstrates the power of this method of analysis and the influence of the different fitting parameters onto the computer-generated line shapes. The findings of the section lead directly to the conclusion that there exists a mass renormalization of the carriers in the condensate and give the first experimental evidence[24-26] for this theoretically predicted effect.[27,28] Section III E contains all empirical data resulting from the line-shape analysis. The most important features are a strong increase of the $e$-$h$ density with increasing field strength and an increase of the ground-state energy but at the same time a constancy of the work function (energy gap to the free-exciton energy). The discussion of these results follows in Sec. IV. A simple way of understanding the newly found properties is presented, followed by a comparison of our data with the various theoretical predictions for the EHL in a magnetic field. In addition we present results of our own calculations. They are based on a new point of view that, in the field range employed, it is the kinetic part of the ground-state energy which is predominantly influenced by the magnetic field, while the sum of exchange and correlation energy is much less affected. Section V presents experimental data on the other phonon replicas appearing in the EHL radiative recombination spectrum, i.e., the EHL (TO) and the EHL (TA) line, that differ in shape from the EHL (LA) line discussed in the previous sections. We show, using the results from the EHL (LA) line, that we can generate the EHL (TA) line shape theoretically at all magnetic-flux densities. Measurements on total luminescence intensities are presented in Sec. VI. Explicit data are given on the field dependence of the ratio of the total intensities of the EHL (TA) and the EHL (LA) line, which increases by more than a factor of 2 over the field range studied. As in the aforementioned case of the shape of the EHL (TA) line the intensity increase is satisfactorily explained by the difference in the $\vec{k}$ dependence of the two recombination processes.

In the conclusion, Sec. VII, we will summarize the spectrum of new results emerging from our studies and will give a prospective on some interesting questions that remain to be settled for the EHL in a magnetic field.

## II. EXPERIMENTAL

The experiments were performed on ultrapure Ge crystals with an impurity concentration of less than $10^{11}$ cm$^{-3}$. The samples were immersed in superfluid He at temperatures between 1.6 and 2 K. Magnetic fields up to 19 T (190 kG) were supplied by a 10-MW Bitter magnet with 50-mm bore. In all experiments, the field was oriented parallel to one of the [100] directions of the crystal, so that the degeneracy of the four conduction-band minima remained unchanged. The samples usually were aligned by visual adjustment of the x-ray oriented crystals, a method that is probably accurate to about 2°. In some cases the alignment was performed by means of far-infrared cyclotron resonance, using an $H_2O$ laser (see also Sec. III). The accuracy of this method is better than 0.1°. The experimental results from samples oriented in both ways did not differ from one another, so that data from both kinds of alignment were used for subsequent analysis. Free carriers were created by a focused argon ion laser. The absorbed power was typically 300 mW. The recombination radiation emerging with wave vector $\vec{k}$ from the electron-hole liquid (EHL) could be detected in Faraday ($\vec{k} \parallel \vec{H}$) as well as in Voigt configuration ($\vec{k} \perp \vec{H}$). In the latter case, a small mirror close to the sample deflected the emitted light towards the exit window at the bottom of the cryostat. The emitted radiation was analyzed with a 1-m grating spectrometer and detected by a cooled PbS cell, whose signal was processed with routine lock-in technique. Different polarizations were selected using either a linear analyzer in Voigt configuration or a circular analyzer, consisting of a Fresnel rhombohedron and a linear polarizer in Faraday configuration.

The depolarization of the EHL radiation before it reaches the detector poses one of the most serious problems in this type of experiment. Preliminary studies showed that the most intense radiation is often emitted from crystal edges and not from the position of the laser spot. Owing to multiple reflections inside the crystal, the mixture of the different light modes ($\sigma^+, \sigma^-, \pi$) leads to completely unpolarized spectra.[24] In order to avoid the collection of light quanta which have been reflected internally, most of the sample surface (dimensions approximately $8 \times 8$ mm$^2$), including the edges, was carefully masked leaving only a circular hole of 1.5 mm in diameter in the middle of the surface. With masked edges the polarization of the EHL luminescence varied only slightly for samples of a great variety of dimensions and shapes (rhombohedrons with parallel, wedged, and uneven surfaces, as well as hemispheres) which should lead to very different conditions for internal reflections. From these results we conclude that we mainly collected directly emitted radiation with an unimportant fraction of internally reflected light.

The presence of impurities seems to suppress the amount of internally reflected light, which we ascribe to impurity-related reabsorption of the luminescence light within the bulk of the sample. So we observed a strong polarization from the luminescence of doped crystals without masking.[24]

## III. LUMINESCENCE SPECTRA OF THE LA REPLICA AND THEIR INTERPRETATION

The indirect band structure of Ge requires the emission of a momentum-conserving phonon during the $e$-$h$ recombination process. Three different lines connected with the emission of TA, LA, and TO phonons can be separated in the experimental spectra.[1] In general, the recombination probability depends in a complicated way on the wave vectors of the three particles involved in the process: $e$, $h$, and phonon. This $k$ dependence of the electron-phonon coupling is a major source of complication for all attempts of interpreting the experimental results. For the LA-assisted recombination, however, group theory establishes the process to be $k$ independent,[29] which, besides its high intensity relative to the other lines, makes the EHL (LA) line most suited for comparison with theoretical predictions on its shape. A slight disadvantage of the EHL (LA) line is its overlap with the very weak EHL (LO) line.[30] Contributions from this underlying line will be neglected throughout this paper but might be partially responsible for some difficulties apparent in the line-shape fit on the low-energy wing.

Figure 1 presents a collective survey of the behavior of the EHL (LA) line under the influence of a magnetic field. This is a three-dimensional plot of the luminescence intensity as a function of photon energy and magnetic-flux density, seen from two different projections. The shape at the front of this "mountain" reproduces the shape of the well-known zero-field EHL (LA) line. Cuts at higher-flux densities yield the luminescence line occurring at those field strengths. The polarization of the line is not yet analyzed in this representation.

The following salient features are noted:

(1) With increasing flux density the line shifts to higher energies.[19]

(2) The smooth line shape in zero field becomes

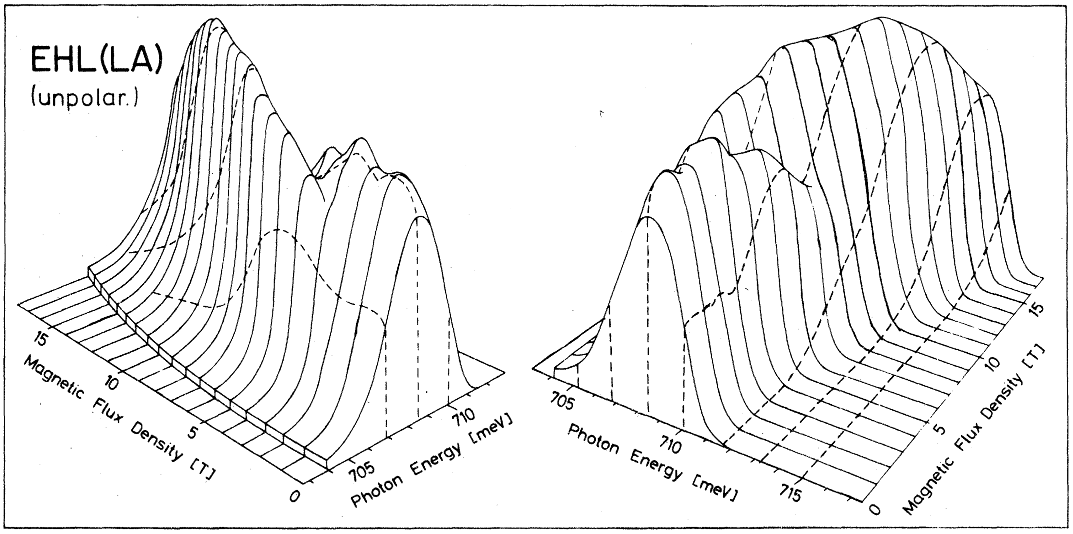


FIG. 1. Survey of the behavior of the EHL (LA) line in a magnetic field. No polarizer was used.

more and more structured. Already at 2 T weak shoulders appear at the low-energy wing. With increasing flux density they become stronger and dominate the line in the high-field region. On the other hand, the marked structures which are present around 3 T in the middle of the line slip down the line in high fields and leave it at the high-energy side. In general, with increasing $H$ new peaks or shoulders appear on the low-energy wing, move across the line, and eventually disappear at the high-energy flank. Structures in the line shape are seen up to the highest fields of 19 T.

(3) The width of the luminescence line (i.e., the sum of the Fermi energies in the valence and conduction band) remains approximately constant over the whole field range.

(4) The total intensity is generally only weakly field dependent (but notice the sharp increase in the range from 0 to 1 T; this is a field range, where a change of the line shape cannot yet be detected).

Figure 2 shows the polarization properties of the EHL (LA) recombination band. The lines have the same overall characteristics as the unpolarized lines in Fig. 1. However, in detail a pronounced difference in the shape can be seen in the various polarizations, even if a complete separation does not occur.

### A. Theory of the line-shape analysis in the absence of a magnetic field

The spectral distribution of the luminescence intensity $I(h\nu)$ for a semiconductor with an indirect band gap is obtained by summing up all possible $e$-$h$ recombination processes that result in the emission of a photon of energy $h\nu$.

$$I(h\nu) \propto \int_{V_e} \int_{V_h} |M_i(\vec{k}_e, \vec{k}_h)|^2 \times \delta(h\nu + \hbar\omega_i - E_g' - E^e_{\text{kin}} - E^h_{\text{kin}}) d\vec{k}_e d\vec{k}_h . \quad (1)$$

Here $\vec{k}_e$, $\vec{k}_h$ and $E^e_{\text{kin}}$, $E^h_{\text{kin}}$ represent wave vectors and kinetic energies of the particles. $\hbar\omega_i$ is the energy of the participating phonon, $E_g'$ the reduced band-gap energy. The integral is taken over the *occupied* $k$-space volumes $V_e$ and $V_h$ (Fermi sta-

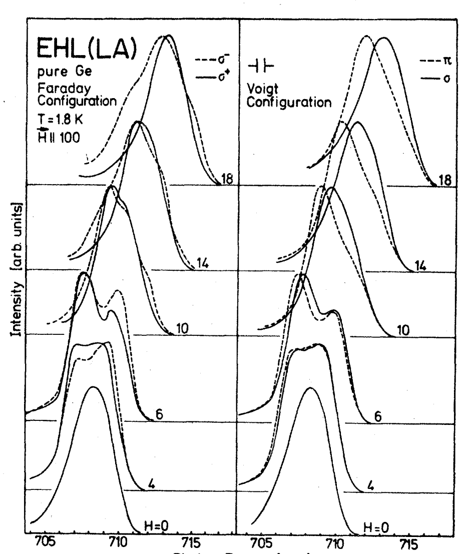


FIG. 2. Polarization of the EHL (LA) line in Faraday and Voigt configuration.

tistics). The $\delta$ function assures energy conservation of the process. The index $i$ distinguishes between the various phonons. The explicit form of the electron-phonon matrix element $M_i(\vec{k}_e,\vec{k}_h)$ is unknown. However, when dealing with highly symmetrical points of the Brillouin zone (i.e., $\Gamma$ point and $L$ point) we can expand the matrix element as

$$M_i(\vec{k}_e,\vec{k}_h)=M_i^0+\vec{M}_i^e\cdot\vec{k}_e+\vec{M}_i^h\cdot\vec{k}_h+\cdots . \tag{2}$$

For the allowed LA transition $M_i^0=M_{\mathrm{LA}}^0$ is finite, and following the usual custom, we assume $M_{\mathrm{LA}}^e$ and $M_{\mathrm{LA}}^h$ to be negligible by comparison. In the case of a forbidden transition, however, $M_i^0$ vanishes and one is compelled to go to the next ($k$-dependent) terms in the expansion (see Sec. V B). When $M_i$ is independent of $\vec{k}$ (allowed transition) it may be taken out of the integral (1) and one obtains the simple one-dimensional convolution integral

$$I(h\nu)\propto |M_{\mathrm{LA}}^0|^2\int_0^\infty D^e(E^e)f(E^e,E_F^e,T)\times D^h(E^h)f(E^h,E_F^h,T)\,dE^e\,, \tag{3}$$

with the simultaneous condition $E^h=h\nu-E^e-E_g'^{\mathrm{LA}}$ ($E_g'^{\mathrm{LA}}=E_g'-\hbar\omega_{\mathrm{LA}}$). Here $D^e(E^e)$ and $D^h(E^h)$ are the densities of states of $e$ and $h$, respectively, $f(E^e,E_F^e,T)$ and $f(E^h,E_F^h,T)$ denote the Fermi distribution function for a temperature $T$ and with Fermi energies $E_F^e$ and $E_F^h$, respectively; $E_g'^{\mathrm{LA}}$ is the reduced band-gap energy $E_g'$ diminished by the energy of the $L$-point LA phonon ($\hbar\omega^{\mathrm{LA}}$). This formula was used by many authors to analyze the line shape of the EHL (LA) recombination line and to extract values for the reduced band-gap energy $E_g'$ and the $e$-$h$ density

$$n=\int_0^\infty D^e(E^e)f(E^e,E_F^e,T)\,dE^e=\int_0^\infty D^h(E^h)f(E^h,E_F^h,T)\,dE^h\,. \tag{4}$$

### B. Theory of the line-shape analysis in the presence of a magnetic field

The analysis of the EHL (LA) spectrum in the presence of a magnetic field is performed in complete analogy to the zero-field case. Again we assume the time for thermalization of the carriers to be much shorter than their lifetime. This meets the experimental fact of not having observed luminescence from hot carriers as in Ge under unaxial stress.[31] To synthesize theoretically the line shape for the various polarizations labeled by the index $p$ in a magnetic field $H$, we write the convolution integral in the following form:

$$I_p(h\nu,H)\propto |M_{\mathrm{LA}}^0|^2\sum_{S_i,M_j}\alpha(S_i,M_j)\delta_{S_i,M_j+p}\times\int_0^\infty D_{S_i}^e(E^e,H)f(E^e,E_F^e(H),T)\times D_{M_j}^h(E^h,H)f(E^h,E_F^h(H),T)\,dE^e\,, \tag{5}$$

with

$$E^h=h\nu-E_g'^{\mathrm{LA}}(H)-E^e\,,$$
$$S_i=\pm\tfrac12\,,\quad M_j=\pm\tfrac12,\ \pm\tfrac32\,,\quad p=0,\pm1\,,$$
$$\delta_{ij}=\begin{cases}0 \text{ for } i\neq j\\ 1 \text{ for } i=j\,.\end{cases}$$

The electron-phonon matrix element $|M_{\mathrm{LA}}|^2$ is assumed to be field, spin, and $k$ independent. $D_{S_i}^e(E^e,H)$ and $D_{M_j}^h(E^h,H)$ are partial densities of states for electrons with magnetic quantum number $S_i=\pm\frac12$ and holes with magnetic quantum number $M_j=\pm\frac32,\pm\frac12$, respectively.[32] Their particular form will be made clear in the following section. The Fermi energies $E_F^e(H)$ and $E_F^h(H)$ as well as the reduced energy gap $E_g'^{\mathrm{LA}}(H)$ now are assumed to be field dependent. The Kronecker symbol guarantees the conservation of the projection of total spin parallel to $H$ for electron plus hole plus photon (for an indirect optical transition there exists no such selection rule on the Landau quantum number).[33] The function $\alpha(S_i,M_j)$ represents the statistical weight for the transition between initial state $S_i$ and final state $M_j$.[33] Again the Fermi energies $E_F^e(H)$ and $E_F^h(H)$ are determined uniquely by the $e$-$h$ pair density $n(H)$ through the equations

$$n(H)=\int_0^\infty D^e(E^e,H)f(E^e,E_F^e(H),T)\,dE^e\,,=\int_0^\infty D^h(E^h,H)f(E^h,E_F^h(H),T)\,dE^h\,, \tag{6}$$

which must be solved iteratively. $D^e$ and $D^h$ are total densities of states resulting from a summation over the partial densities of states in each of the bands

$$D^e(E^e,H)=\sum_{S_i}D_{S_i}^e(E^e,H)$$

and

$$D^h(E^h,H)=\sum_{M_j}D_{M_j}^h(E^h,H)\,.$$

The integral (5) can be reduced to

$$I_p(h\nu,H)\propto |M_{\mathrm{LA}}|^2\bigg[\beta(p)\int_0^\infty D_{1/2}^e(E^e,H)f(E^e,E_F^e(H),T)\times D_{1/2+p}^h(E^h,H)f(E^h,E_F^h(H),T)\,dE^e+\gamma(p)\int_0^\infty D_{-1/2}^e(E^e,H)f(E^e,E_F^e(H),T)\times D_{-1/2+p}^h(E^h,H)f(E^h,E_F^h(H),T)\,dE^e\bigg], \tag{7}$$

where $E^h = h\nu - E_g^{\prime\mathrm{LA}}(H) - E^e$. The quantities $\beta(p)$ and $\gamma(p)$ are listed in the following table:

| $p$ | Polarization | $\beta(p)$ | $\gamma(p)$ |
|---|---|---|---|
| 0 | $\pi$ | $\frac{1}{2}$ | $\frac{1}{2}$ |
| +1 | $\sigma^+$ | $\frac{3}{4}$ | $\frac{1}{4}$ |
| −1 | $\sigma^-$ | $\frac{1}{4}$ | $\frac{3}{4}$ |

For a given polarization index $p$, there remains the sum of two convolution integrals: the first one treating all possible recombinations of electrons with spin projection $S_t = \frac{1}{2}$ with holes of spin projection $M_j = +\frac{1}{2} + p$, the second one treating all those of electrons with spin projection $S_t = -\frac{1}{2}$ with holes of spin projection $M_j = -\frac{1}{2} + p$. In both cases a photon with angular momentum $p = -1, 0, +1$ relative to the magnetic-field direction is emitted.

The fundamental condition for the performance of the analysis is the detailed knowledge of the density of states $D^e_{St}$ and $D^h_{M_j}$ for Ge in the presence of a magnetic field.

### *1. Density of states of the conduction band*

The lowest conduction band of Ge is constituted by four minima at the $L$ points of the Brillouin zone with spheroids as surfaces of constant energy. The density of states of the conduction band with a magnetic field applied along the [100] direction can be written in analogy to a formula given in Ref. 34:

$$D^e_{\pm 1/2}(E^e, H) = 4\frac{1}{2\pi l^2}\frac{1}{2\pi}\left(\frac{2m_s^*}{\hbar^2}\right)^{1/2} \times \sum_n \left[E^e - \left((2n+1)\frac{m_0}{m_c^*} \pm \frac{g}{2}\right)\mu_B H\right]^{-1/2} \tag{8}$$

with

$$\frac{1}{l^2} = \frac{eH}{\hbar c}.$$

The effective mass in the $\vec{\mathrm{H}}$ direction is[35]

$$m_s^* = m_l^* \cos^2\Theta + m_t^* \sin^2\Theta$$

and the cyclotron mass is[36]

$$\left(\frac{1}{m_c^*}\right)^2 = \frac{\cos^2\Theta}{m_t^{*2}} + \frac{\sin^2\Theta}{m_l^* m_t^*}.$$

For the longitudinal and transverse mass we use[37]

$$m_l^* = 1.588 m_0$$

and

$$m_t^* = 0.08152 m_0,$$

and the angle $\Theta$ is

$$\Theta = \arccos(1/\sqrt{3}) \text{ for } \vec{\mathrm{H}} \parallel [100].$$

This yields

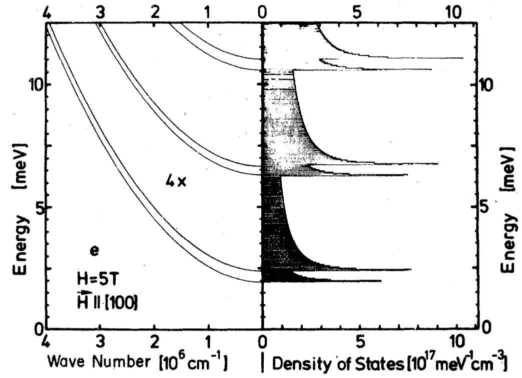


FIG. 3. Dispersion relation and density of states of the conduction band of Ge, computed for a magnetic field of 5 T parallel to the [100] direction of the crystal.

$$m_s^* = 0.5837 m_0,$$

$$m_c^* = 0.1345 m_0.$$

For the $g$ factor of the electrons we use[38]

$$g = 1.57.$$

Bohr's magneton is denoted by

$$\mu_B = \frac{e\hbar}{2m_0 c}$$

and the Landau quantum number by

$$n = 0, 1, 2, \ldots.$$

The factor 4 appears because of the energetic degeneracy of the four conduction-band minima. The term $1/l^2$ describes the degeneracy of states in $k$ space in the plane perpendicular to the field $(k_x, k_y)$. The rest of formula (8) is a sum over the density of states of one-dimensional bands, labeled by the Landau quantum number $n$, beginning at energies $E_{n\pm} = [(2n+1)(m_0/m^*) \pm g/2]\mu_B H$. The summation extends over all $n$ for which the square-root term remains real. A plot of the density of states and the $E(k)$ relation is presented in Fig. 3 for a magnetic field of 5 T parallel to the [100] direction of the crystal.

### *2. Density of states of the valence band*

In zero field, the top of the $\Gamma'_{25}$ valence band of Ge is fourfold degenerate, leading to a complicated splitting under the influence of a magnetic field.[16,17,39] The dispersion of the Landau levels can be evaluated only numerically. Recently, this computation has been done taking Ge as a model substance by J.C. Hensel and K. Suzuki,[17] who also verified their theoretical results experimentally. Figure 4 shows the dispersion of the Landau levels in a field of 5 T. The plot was calculated by diagonalizing the secular matrix of the problem, trun-

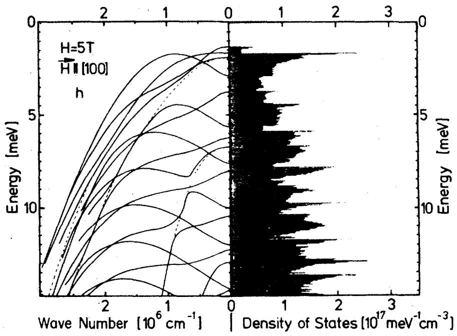


FIG. 4. Dispersion relation and density of states of the valence band of Ge, computed for a magnetic field of 5 T parallel to the [100] direction of the crystal. The dispersion relation was taken from the work of Hensel and Suzuki (Ref. 17).

cated to a dimension of 80×80 in small steps for 400 fixed values of $k_H$ (the wave vector along the field direction). The usual functions,

$$\Psi_{n,M_j}(k_H)=u_n|k_H,M_j\rangle ,\quad n=0,1,2,\ldots ,\quad M_j=\pm\tfrac{1}{2},\ \pm\tfrac{3}{2} \tag{9}$$

a product of an oscillator function $u_n$ and a Bloch function $|k_H,M_j\rangle$ with spin projection $M_j$, served as a basis. For each $k_H$, the diagonalization resulted in 80 eigenvalues $E_m(k_H)$ and 80 eigenstates

$$\phi_m(k_H)=\sum_n\sum_{M_j}a_n(k_H,M_j)u_n|k_H,M_j\rangle , \tag{10}$$

which are linear combinations of the basis functions with coefficients $a_n(k_H,M_j)$.

Thus an individual eigenstate $\phi_m(k_H)$ is composed of a linear combination of the four spin projections $M_j$, each contributing with a weight of

$$g_{mk_H}(M_j)=\sum_n|a_n(k_H,M_j)|^2\leq 1 ,\quad M_j=\pm\tfrac{1}{2},\ \pm\tfrac{3}{2} \tag{11}$$

where

$$\sum_{M_j}g_{mk_H}(M_j)\equiv 1 .$$

Using the recorded unpublished results for $E_m(k_H)$ and $\phi_m(k_H)$ from Ref. 17, we evaluated numerically the four partial densities of states of the valence band corresponding to $M_j=\pm\frac{1}{2},\ \pm\frac{3}{2}$. The result is presented in Fig. 5. The total density of states as given by $D^h(E^h)=\sum_{M_j}D^h_{M_j}(E^h)$ is shown in Fig. 4.

### 3. Nonparabolicities of the bands

In the calculation of the density of states near the extrema of the bands, all relevant energies are assumed to vary linearly with the magnetic-flux density, i.e., nonparabolicities of the bands

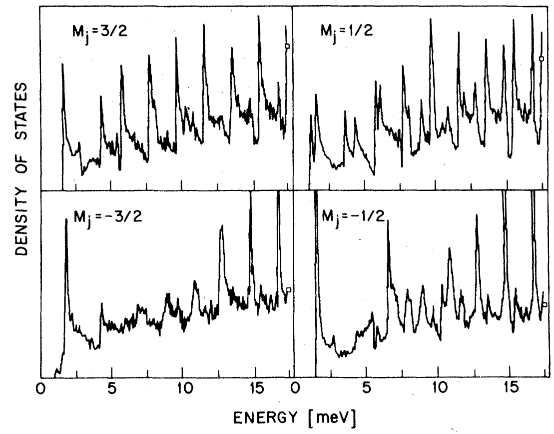


FIG. 5. Density of states of the valence band of Ge in a magnetic field of 5 T parallel to the [100] direction. The four quadrants illustrate the distribution of the density of states among the four different magnetic quantum numbers.

are not taken into account. This approximation needs the following justification:

(1) *Conduction band*. The energy of the highest populated state in the EHL at maximum field (19 T) is less than 10 meV above the band edge at $H=0$. For such energies, the mass increase due to nonparabolicities is less than 1%,[40] which is out of range of the sensitivity of our line-shape analysis.

(2) *Valence band*. Numerical calculations of the valence-band Landau levels, using the program of Pidgeon and Brown,[41] which includes explicitly the interactions of the valence band with the conduction band and the spin-orbit split-off band, show a maximum deviation from linearity of less than 3% at 19 T (and considerably less at lower fields).[42] The deviations at $k_H\neq 0$ are assumed to be of the same magnitude.

### 4. Lifetime broadening of the levels

The simple theory we have outlined above predicts that the low-energy side of the line shape in the presence of the highest fields applied approaches a step function from zero to maximum intensity corresponding to the singular nature of the one-dimensional densities of states. In actual fact, however, at fields above 8 T the EHL luminescence line shows a low-energy tail of almost exactly Lorentzian shape. Therefore there must exist a broadening mechanism that smears out these singularities. This finding led us to apply a model earlier suggested by P.T. Landsberg[43,44] to describe the low-energy tail of x-ray fluorescence of simple metals to the recombination spectra of EHL. (This model has successfully been used to describe the low-energy tail of the

EHL spectra in the absence of a magnetic field, too.[45]) Following Landsberg, each state in the band has to be replaced by a Lorentzian distribution of half-width $\Gamma = \hbar/\tau$ over all neighboring states. $\tau$ is the quasiparticle lifetime, i.e., the lifetime of the two vacancies that are left in the Fermi seas of electrons and holes, respectively, after the recombination process. The half-width $\Gamma(E)$ of the replaced states of each band is a complicated function of energy, which has a maximum $\Gamma_0$ at the band edges and decreases monotonically to zero when $E$ approaches the Fermi level. While this result was derived for the case of three-dimensional, isotropic, parabolic, nondegenerate bands, which strictly speaking does not correspond to our situation, nevertheless we believe that the result is sufficiently general that the basic properties are not much changed, i.e., we expect a maximum broadening $\Gamma_0(H)$ at the bottom of the bands and $\Gamma(E)$ to be zero at the Fermi level. Several test calculations, trying various monotonically decreasing interpolation schemes between these two fixed points actually resulted in slightly different theoretical EHL line shapes, but the positions of the characteristic structures were not influenced. Therefore, we adopted the simplest of those interpolation functions

$$\Gamma(E,H) = \Gamma_0(H)\left(1 - \frac{E}{E_F(H)}\right) \tag{12}$$

for all future analyses. The replacement of the discrete energy states by a broadened level of half-width $\Gamma(E)$ leads to a modified density of states which is given for the electrons by

$$D^{e*}_{S_t}(E^e,H) = \int_0^\infty \tilde{L}(E^e,E^e_1) D^e_{S_t}(E^e_1,H)\,dE^e_1 , \tag{13}$$

with

$$\tilde{L}(E^e,E^e_1) = \begin{cases} L(E^e,E^e_1) & \text{for } E^e_1 < E^e_F \\ \delta(E^e - E^e_1) & \text{for } E^e_1 \geq E^e_F , \end{cases}$$

$$L(E^e,E^e_1) = \frac{1}{2\pi}\,\frac{\Gamma(E^e_1)}{(E^e - E^e_1)^2 + [\Gamma(E^e_1)/2]^2} .$$

Analogous expressions hold for the densities of states of the holes. As in the zero-field case,[45] the same broadening parameter $\Gamma_0(H) = \Gamma^e_0(H) = \Gamma^h_0(H)$ has been used for electrons and holes. Figure 6 illustrates the procedure described here, using the total density of states at 5 T as an example.

For the actual calculation of the line shape, the partial densities of states $D^e_{S_t}(E^e,H)$ and $D^h_{M_j}(E^h,H)$ in the convolution integral (7) have to be replaced by their broadened counterparts $D^{e*}_{S_t}(E^e,H)$ and $D^{h*}_{M_j}(E^h,H)$. In addition to the broadening mechanism described above there will be higher-order distortions to the line shape; e.g., a plasmon satellite.[28] We will neglect those contributions in our analysis.

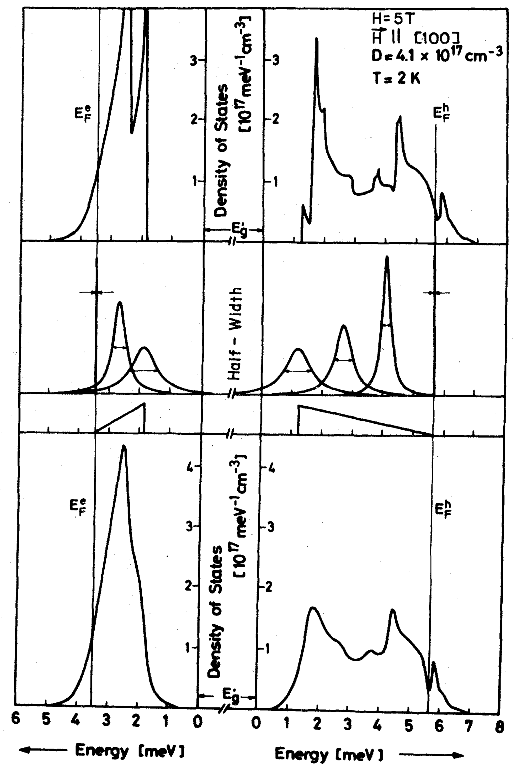


FIG. 6. Illustration of the effect of level broadening on the density of states for the case of $H = 5$ T in the [100] direction: (a) unbroadened density of states times Fermi distribution function, (b) schematic sketch of the Lorentz function which is convolved with the density of states function from (a), (c) energy dependence of the halfwidth of the Lorentz function, (d) resulting density of states times Fermi distribution function after performance of the level broadening.

### C. Numerical calculation of the line shape

To sum up the foregoing discussion we note that there are only three adjustable parameters left for the analysis of the EHL (LA) line shape in a given magnetic field, and one set of parameters has to reproduce the line shapes of all four senses of polarization. The free parameters are as follows:

(1) the electron-hole density $n(H)$ that determines the Fermi energies via Eq. (6),

(2) the broadening parameter $\Gamma_0(H)$ of Eqs. (12) and (13), and

(3) the electron temperature $T$[46] that is completely determined by the high-energy cutoff of the line and shows no field dependence.

($E_g'^{LA}$ is not determined from the line shape, but from its position on the energy scale and can easily be deduced after experimental and theoretical shape have reached good agreement.)

By appropriately choosing the electron-hole density $n(H)$ and the broadening parameter $\Gamma_0^e(H) = \Gamma_0^h(H)$ at each given magnetic field we were able in all cases to obtain good agreement between theoretical and experimental line shapes. The procedure is illustrated in Fig. 7 for line shapes measured at 5 T. For reference we show in Fig. 8 the conduction- and valence-band densities of *occupied* states for trial values of $e$-$h$ densities used for the fitting process in Fig. 7.

In Fig. 7(a) we start out with the zero-field value of the electron-hole density $n = 2.2\times10^{17}$ cm$^{-3}$. The resulting theoretical line is much too narrow and does not show the characteristic double structure of the experimental result. In Fig. 7(b) the density is increased substantially to $n = 3.9\times10^{17}$ cm$^{-3}$. Now the characteristic features of the line are well reproduced; however, the theoretical line is about 10% too broad with respect to the experimental data. Figure 7(c) shows an attempt to produce the correct linewidth by reducing the density (and in turn the Fermi energies) to a value of $n = 3.2\times10^{17}$ cm$^{-3}$. However, although producing the correct linewidth, this reduction in density distorts the line considerably.

Figures 7(b) and 7(c) in conjunction with Fig. 8 demonstrate an essential feature of the line-shape analysis in the presence of a magnetic field. In contrast to the 0-field case, the electron-hole density is *not* determined from the width of the line but from the structures on the line, which determine the position of the Fermi energy with re-

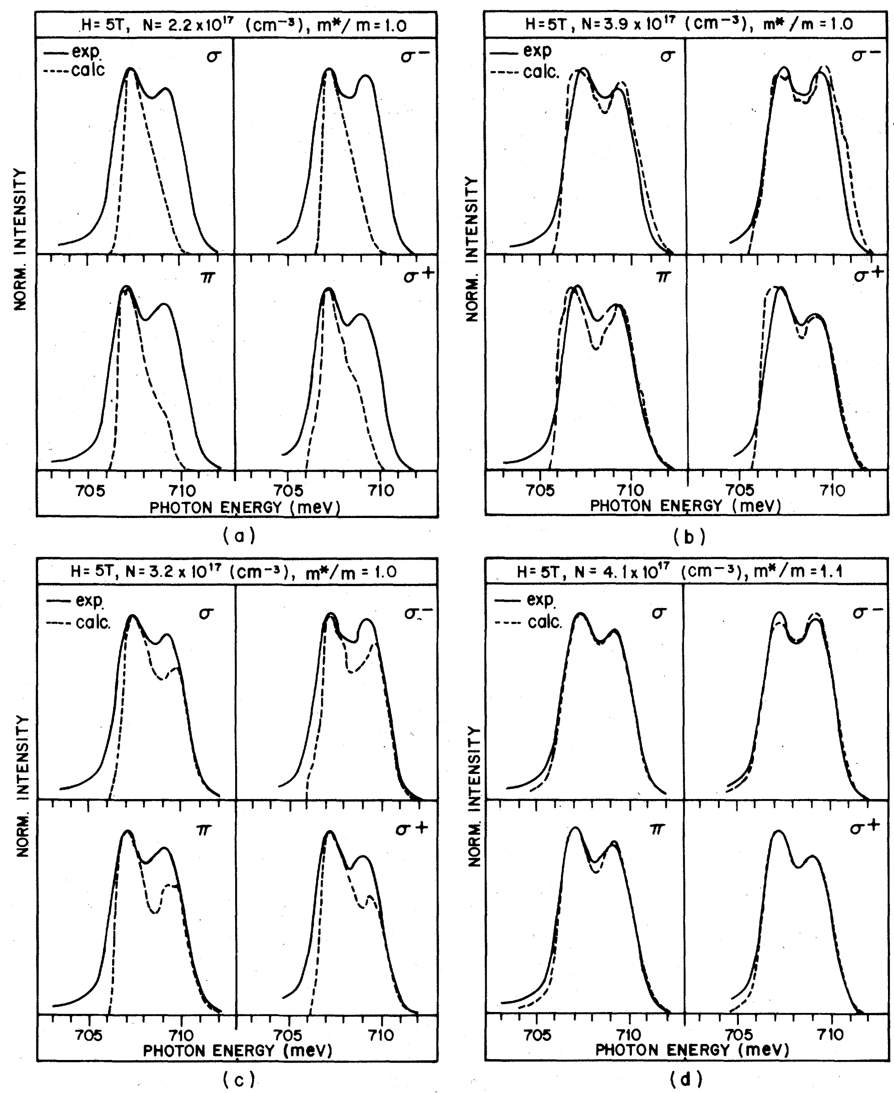


FIG. 7. Comparison of experimental and theoretical EHL (LA) line shape at $H = 5$ T in all four modes of polarization, computed for various $e$-$h$ densities. $m^*/m$ denotes mass enhancement. For detailed explanation refer to text.

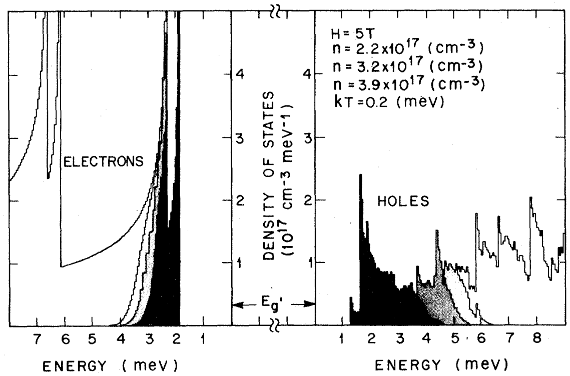


FIG. 8. Degree of population of the densities of states for conduction and valence bands at 5 T for the densities used in Fig. 7. For simplicity the total densities of states are shown.

spect to the characteristic peaks in the densities of states of Fig. 8.[47]

From the above it is evident that there is little latitude in determining the *e-h* density; the optimum fit to the line shape requires that a second peak in the valence-band density of states (see Fig 8) be occupied in order to produce the observed structure. Thus we tentatively fix the value of the density (at each given field) by optimizing the fit to the *structure*. However, we are left with an unsatisfying discrepancy in the linewidth. This is especially disturbing in view of the fact that this discrepancy is seen in every case analyzed over the entire field range from 2 to 19 T.

### D. Mass renormalization

In order to bring the theoretically generated linewidth into agreement with the experimental one we are forced to look beyond the standard approach we have used up to this point. An almost perfect agreement between theoretical and experimental line shape can be achieved if we use a reduced energy scale for the plot of the calculated line, i.e., compressing the line by approximately 10%. Such a scale reduction implies a reduction of the energy scale of the densities of states shown in Fig. 8 as well. This in turn is formally equivalent to an increase of the cyclotron masses of the carriers by a factor of $\xi = 1.1$. (This is readily understood recalling that the energy inferred between singularities in a simple band is reciprocally proportional to the cyclotron mass.) From there we conclude that the apparent scale reduction demonstrates a renormalization of the carrier masses of the EHL being approximately 1.1 times heavier than the one-particle band masses, which were the basis for the calculation of the densities of states.

The degree of agreement that can be established between theory and experiment under the assumption of a mass renormalization of $\xi = 1.1$ is shown in Fig. 7(d). We now also include the finite quasiparticle lifetime via the broadening parameters $\Gamma_0$,[48] which rounds off the edges but does not influence the position of the structures on the line. We see that the fit is excellent.

In the same way all experimental EHL (LA) lines have been synthesized numerically from the "compressed" densities of states for electrons and holes. Some selected examples are presented in Fig. 9. Good agreement was found in all 14 cases of magnetic field strength analyzed. Finally, these line-shape fits yielded the field dependence of all characteristic parameters of the condensate (see Sec. III E).

A possible field dependence of the renormalization parameter $\xi$ cannot be excluded. There exists a mutual dependence among the parameters $n(H)$, $\Gamma_0(H)$, and $\xi$ that makes it possible to create similar line shapes with slightly different sets of parameters. However, from all the curves we synthesized, we conclude that the uncertainty in $\xi$ is less than 5% so that $1.05 \leq \xi \leq 1.15$. While a field dependence within these limits is conceivable,[49] nevertheless, we assume the mass renormalization factor to be field independent, $\xi = 1.1$, in order to avoid introducing another field-dependent adjustable parameter.

This analysis of the luminescence line shape in the presence of a magnetic field gave the first experimental evidence[50] for the predicted mass enhancement.[27] In the meantime a mass renormalization was also found by Gavrilenko *et al.*[26] from magnetoplasma resonance experiments.

### E. Field dependence of the EHL parameters

Our line-shape analysis, presented in the foregoing chapter, yields the first consistent set of data on the field dependence (up to 19 T) of most of the EHL parameters. Those parameters are as follows:

(1) the ground-state energy $E_G(H)$,
(2) the reduced band-gap energy $E_g'^{\,\mathrm{LA}}(H)$,
(3) the chemical potential $\mu^{\mathrm{LA}}(H)$,
(4) the Fermi energy $E_F(H) = E_F^e(H) + E_F^h(H) = \mu^{\mathrm{LA}}(H) - E_g'^{\,\mathrm{LA}}(H)$,
(5) the work function $\phi(H)$,
(6) the electron hole density $n(H)$, and
(7) the broadening parameter $\Gamma_0(H)$, a measure for the quasiparticle lifetime.

All this empirical information is summarized in Figs. 10 to 13. The values for the parameters (1) through (5) of the list above, as they result from

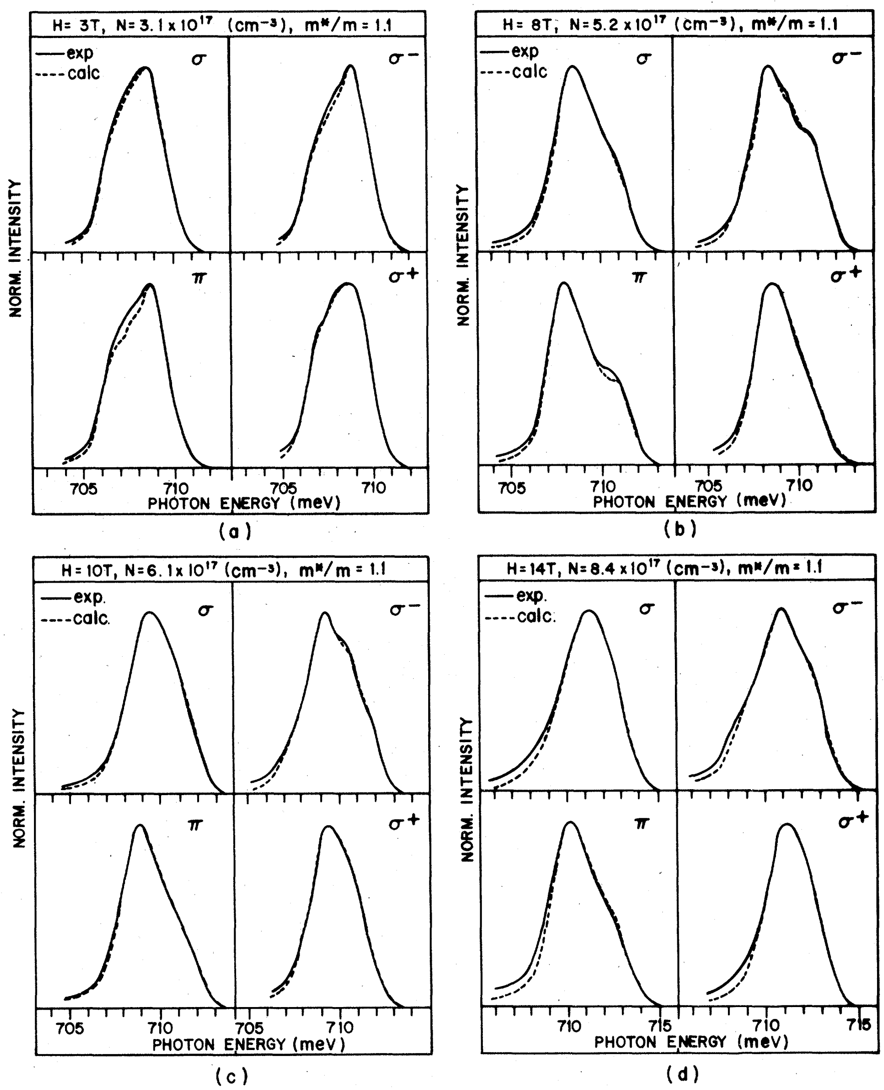


FIG. 9. Comparison of experimental and theoretical EHL (LA) line shape for various flux densities in all four modes of polarization, computed with 10% mass enhancement and lifetime broadening of the levels.

our line-shape analysis procedure, can directly be taken from Fig. 10. The ground-state energy $E_G(H)$ is repeated separately in Fig. 11. (LA denotes in all cases an energy reduction by one-LA-phonon energy.) The shaded area marks the energy range of EHL (LA) luminescence, bounded by the chemical potential $\mu^{\mathrm{LA}}(H)$ and the reduced band-gap energy $E_g'^{\mathrm{LA}}(H)$. (In reality EHL (LA) luminescence appears slightly beyond these boundaries owing to thermal broadening at the high-energy side and the quasiparticle lifetime at the low-energy side.) The data points labeled $\mathrm{E}_{\mathrm{FE}}^{\mathrm{LA}}$ represent the position of the peak of the free-exciton luminescence. The FE line was measured without a polarizer at $T = 4.2$ K. No line-shape analysis was performed for the free exciton.[51] The upper straight line of Fig. 10 denotes the variation of the indirect band gap as determined from the edges of the calculated densities of states for electrons and holes.

The data points in Fig. 12 show the electron-hole density of the condensate versus magnetic-flux density, assuming a field-independent mass renormalization of 10%. Figure 13 illustrates the field dependence of the broadening parameters $\Gamma_0(H) = \Gamma_0^e(H) = \Gamma_0^h(H)$.

## IV. DISCUSSION OF RESULTS

The success of our line-shape analysis proves that the shape of the recombination spectrum of the electron-hole liquid in Ge in the presence of a magnetic field can be understood on the basis of the single-particle dispersion relation of its constituents with a slight renormalization of their masses. The conclusion that a mass renormaliza-

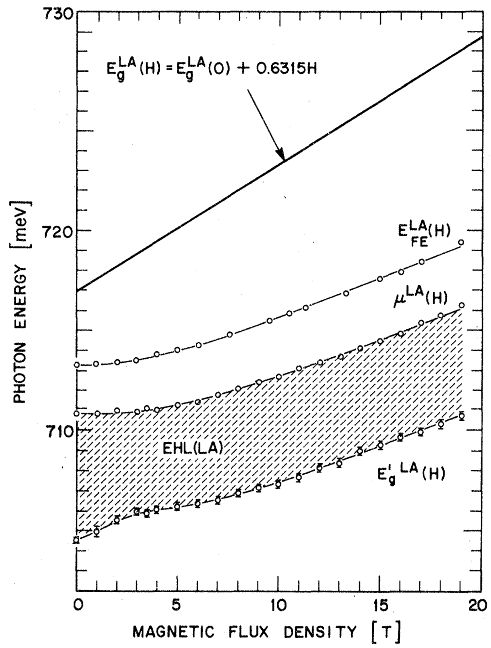


FIG. 10. Field dependence of the characteristic EHL parameters. Both the chemical potential $\mu^{LA}$ and the reduced band gap $E_g'^{LA}$ were yielded by the line-shape analyses. The points $E_{FE}^{LA}$ mark the position of the line maximum of the free-exciton luminescence. The variation of the band gap is calculated using the proportionality factor 0.6315 meV/T.

tion exists can only be drawn from the EHL line-shape analysis in the presence of a magnetic field (for which there arises the apparent contradiction between linewidth and line structure). However, from a reliable determination of $\xi$ (=1.1) at the relatively small field of 3 T and from its weak dependence on field strength, we conclude that a re-

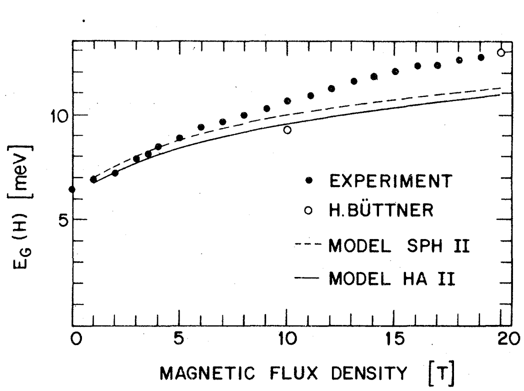


FIG. 11. Field dependence of the ground-state energy $E_G$ in comparison with the results of our theoretical calculation using two different functions for the correlation energy taken from Ref. 70 (SPH II is a self-consistent particle-hole approximation, HA II is a Hubbart approximation). The points ○ are taken from Ref. 14.

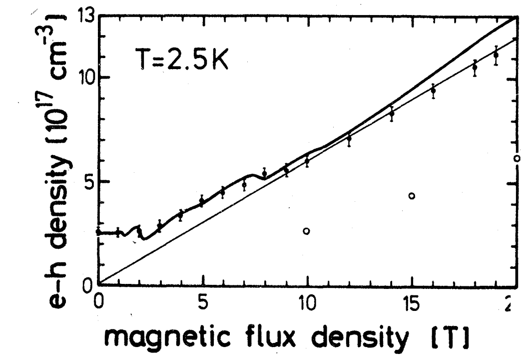


FIG. 12. Electron-hole density as a function of the magnetic-flux density. The values are obtained from the line-shape analyses including a mass renormalization of 10%. The straight line through the origin has a slope of $6\times10^{16}$ cm$^{-3}$ T$^{-1}$ and describes well the behavior of the $e$-$h$ density in the high-field region. The curved line results from our theoretical calculation presented in Sec. IV and Appendix A. The points ○ are taken from Ref. 14.

normalization is present even at zero field. A mass renormalization in the EHL in zero field has been predicted by Rice[27] and Rösler and Zimmermann.[28] The theoretical values of $\xi$ are anisotropic and differ for electrons and holes.[27] They cover a range from $\xi = 1.0$ to 1.1 for electrons and $\xi = 1.1$ to 1.15 for holes. Our analysis is neither capable of confirming an angular dependence nor distinguishing differences in the renormalization between electrons and holes. However, our experimental value of $1.05 \leq \xi \leq 1.15$ confirms the magnitude of the theoretical predictions.

Taking $\xi$ to be 1.1 in zero field, where by a line-shape analysis a mass renormalization by $\xi$ is indistinguishable from a density change by $\xi^{3/2}$, we find that the actual electron-hole density in the absence of a magnetic field is approximately 15% higher than has been deduced so far from all zero-field line-shape analyses.

The strong increase of the $e$-$h$ density with increasing field is an important fact. Already in the field region from 0 to 5 T, where most of the mag-

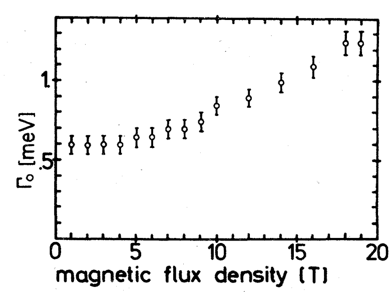


FIG. 13. Field dependence of the broadening parameter $\Gamma_0$ at the bottom of the bands [see Eq. (12)].

neto-oscillatory effects were recorded, a density increase of approximately 50% occurs. This should be taken into account in all future interpretations of magneto-oscillatory data.[52] Another point to notice is the independence (within accuracy of the experiment) of the work function of the EHL[2,4,11] (see Fig. 10). The constant work function raises the interesting question that remains to be answered. Why is it that the energy of the two-particle system, exciton, and the many-particle system, EHL, behave energetically so similar under the influence of a magnetic field?

The field dependence of the broadening parameter $\Gamma_0(H)$ presented in Fig. 13 is in accord with the increasing carrier density. A quantitative understanding, as in the absence of a magnetic field,[45] however, cannot be presented. It would require reconsideration of the possibilities for Auger processes within and between Landau levels of the liquid in the presence of magnetic field.[53]

Let us now try to understand the field dependence of the ground-state parameters of the EHL. Given the variation of the indirect band-gap energy $E_g^{\mathrm{LA}}(H)$ with magnetic field and given the value $\xi$ for the mass renormalization, then the shape and energy position of the EHL line is essentially determined by only two parameters:[54] the ground-state energy $E_G(H)$ and the electron-hole density $n(H)$. [Note the interrelation between Fermi energies $E_F(H)$ and density $n(H)$, and reduced band-gap $E_g'^{\mathrm{LA}}(H)$ and ground-state energy $E_g(H)$]. The main characteristics of the electron-hole liquid under the influence of a magnetic field, therefore, are given in terms of $E_G(H)$ and $n(H)$.

As Fig. 11 shows, the ground-state energy $|E_G| = E_g - \mu$ increases by more than a factor of 2 when the magnetic field is raised from 0 to 19 T, i.e., the condensed state becomes increasingly favored with respect to free electrons and holes. Over the same field range Fig. 12 reveals an increase in the density of approximately a factor of 4 through the width of the EHL (LA) line (a measure of the $e$-$h$ density in zero field) varies only slightly. These features will be discussed in detail in the context of our theoretical model, but can be understood in terms of very simple arguments. The density of states is locally increased at the bottom of the bands, owing to the formation of singularities. This leads to a reduction of the average kinetic energy, $E_{\mathrm{kin}}$, per $e$-$h$ pair of the liquid. If we assume that the sum of the exchange and correlation energy part $E_{xc}$ is not strongly affected by the magnetic field, then the ground state will be shifted in position to lower energy and higher density. An increase in the density, on the other hand, causes an increase (attractive) in $E_{xc} = E_x + E_c$ which in turn lowers the ground-state energy of the condensate, i.e., increases $|E_G(H)|$. Therefore, the field dependence of the ground-state parameters $E_G(H)$ and $n(H)$ originates from the change in the densities of states induces by the application of a magnetic field.

So far, four theoretical calculations for the field dependence of the ground-state parameters of the EHL exist.[14,15,55,56] The only low-field calculation[56] results in predictions for the oscillatory behavior of the total intensity (see also Sec. VI) whose amplitude diverges from experiment[5] by about a factor of 10, which casts doubt on the applicability of the theoretical model used. The three other theories represent high-field approaches to the problem, assuming that all carriers are condensed into their lowest Landau level and lowest spin state. In this extreme quantum limit the field dependence of all three contributions to the ground-state energy $E_{\mathrm{kin}}$ $E_x$, and $E_c$ can be evaluated within well-known approximation schemes. This aim, however, can only be achieved on the basis of a considerable simplification of the valence-band dispersion. In practice this idealization cannot be approached in Ge at the present time. Even in the highest magnetic field available, four Landau levels of the valence band still are populated, leading to a far more complicated situation.

We have performed calculations for the ground-state energy based on a simple model[57] which seems to be applicable to the magnetic-field regime appropriate to our experiments. As we know the actual densities of states of the bands, we can treat the field dependence of the kinetic energy accurately. Exchange and correlation energy, however, can not be calculated in a simple manner. Therefore, we made the not unreasonable assumption that the energy contribution $E_{xc} = E_x + E_c$ is not explicitly dependent on magnetic field. The details are presented in Appendix A and the results are included in Figs. 11 and 12.

The calculated field dependence of the equilibrium density shows very good agreement with our data. The strong increase of the electron-hole density is well reproduced with slight deviations at the very highest fields employed. The occurrence of oscillations in the theoretical curve cannot be confirmed by our present data because of their relatively large uncertainty. However, the existence of these oscillations in the density has been indirectly proven by measurements of the field dependence of the total luminescence intensity performed by Betzler *et al.*[5,6] and by ourselves. They are, in fact, the origin of most of the magneto-oscillatory effects discovered earlier.[58,2-13]

The field dependence of the ground-state energy $|E_G(H)|$ in Fig. 11 is less well reproduced by our model. A considerable deviation from the experimental findings start around 7 to 8 T. However, the general trend of an increasing ground-state energy is found. A possible explanation for this deviation in higher fields can be found in the increasing spin polarization of the electrons, leading to a strong increase of the exchange energy and in turn to an increase of the ground-state energy $|E_G|$. Figures 11 and 12 include the theoretical results of Ref. 14 which show even larger deviations than ours from the experimental findings.[59] We did not include the theoretical predictions of Ref. 55. These values deviate by a factor of 2 to 10 from experiment. However, these authors succeeded in obtaining simple analytic expressions for the field dependence of ground-state energy and density, i.e., $E_G \propto H^{2/7}$ and $n \propto H^{8/7}$, which, if scaled by an appropriate factor, follow our data remarkably well. The scaling factor, however, cannot be derived in any simple way.

In summary, the results of our model calculation for the ground-state parameters of the $e$-$h$ condensate yield satisfactory agreement with the experimental data for

(1) the $e$-$h$ density in the whole magnetic-field range and

(2) the ground-state energy in fields up to about 8 T.

Therefore we conclude that the assumption that exchange plus correlation energy being predominantly density dependent and only weakly field dependent holds true for a very large field range.

## V. OTHER LUMINESCENCE SPECTRA

### A. Experimental result on the EHL (TA) and the EHL (TO) line

We turn now to the remaining EHL luminescence lines in the spectrum. Figure 14 shows the experimental spectra of the EHL (TA) and the EHL (TO) line in comparison with the EHL (LA) results. These spectra were recorded in the Voigt configuration without a polarizer because of the weaker intensity of the TA and TO emission.

Let us first consider the TA line. Similar to the results in the absence of a magnetic field,[60,61] the TA replica of the condensate luminescence has a smaller width than the LA replica. For a given field the structures on the low-energy side are always less pronounced than those of the EHL (LA) line. This can be understood from the $\vec{k}$ dependence of the electron-phonon matrix element for the TA-phonon-assisted radiative recombination [see Eq. (2)]. Generally speaking, structures at the low-energy side of the luminescence line originate from the recombination of electrons and holes that in $\vec{k}$ space are situated nearer to the $L$ point and $\Gamma$ point, respectively, than carriers whose recombination radiation attributes to the high-energy part. The recombination probability decreases with decreasing distance of the carriers from the symmetry points. Therefore, the intensity at the low-energy side of the luminescence line is reduced. As to the EHL (TO) luminescence in Fig. 14, we see a line shape that looks like a mixture of the shape of the allowed (LA) and the forbidden (TA) recombination. This intermediate behavior of the EHL (TO) line in a magnetic field confirms the earlier findings for the zero-field line shape of the EHL (TO) band and group-theoretical consideration on the recombination process.[29,62] For the TO-assisted recombination the $k$-independent term [such as EHL (LA)] and the $k$-dependent term [such as EHL (TA)] are comparable. The field dependence of the EHL (TO) line was not further investigated.

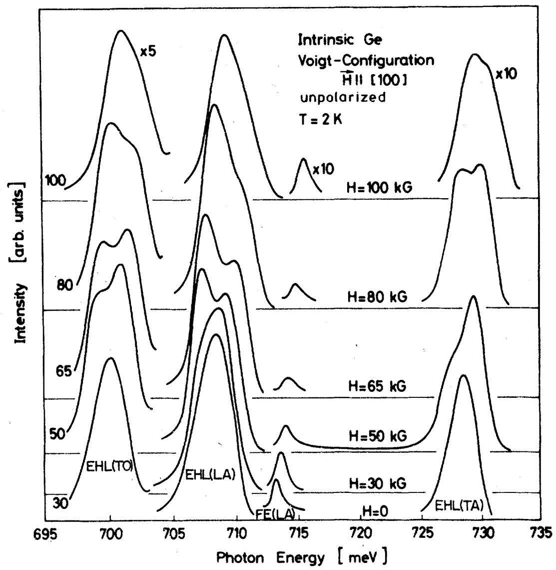


FIG. 14. Complete EHL spectra including TA-, LA-, and TO-phonon lines at different flux densities between 0 and 10 T. The spectra were recorded without a polarizer.

### B. Line-shape analysis of the EHL (TA) line

The electron-phonon matrix element $M_{TA}$ for TA-phonon-assisted recombination processes has been written by Bénoit à la Guillaume *et al.*[60] in the following manner:

$$M_{TA}(\vec{k}_e, \vec{k}_h) = \vec{M}_e \cdot \vec{k}_e + \vec{M}_h \cdot \vec{k}_h + \cdots . \quad (14)$$

However, it can be shown group theoretically that the most effective transition channel via the $\Gamma_2^-$ conduction-band minimum is forbidden for all electrons and holes located along the $\Lambda$ line.[61,62] Therefore, only the components of the wave vectors perpendicular to the $\Lambda$ line ($k_{e\perp}, k_{h\perp}$) have an effect on the transition probability. The matrix element may therefore be written as

$$M_{\mathrm{TA}}(\vec{k}_e, \vec{k}_h) = M^e_{\mathrm{TA}} k_{e\perp} + M^h_{\mathrm{TA}} k_{h\perp} . \tag{15}$$

In case of the holes being near the $\Gamma$ point, where the four $\Lambda$ lines meet, we have to take the sum of the individual recombination probabilities with electrons from all four valleys, i.e., we have to sum over $k^2_{h\perp}$ to all four $\Lambda$ lines. This can be shown to be proportional to $k^2_h$.

Therefore, neglecting higher orders, the electron-phonon matrix element turns out to be

$$M_{\mathrm{TA}}(\vec{k}_e, \vec{k}_h) = M^e_{\mathrm{TA}} k_{e\perp} + M^h_{\mathrm{TA}} k_h . \tag{16}$$

To simplify the calculation we treated only the two extreme cases of coupling for the purpose of our theoretical line-shape analysis, where one term or the other of the sum of Eq. (16) can be neglected. The expression for the EHL (TA) line shape becomes:

$$I_p(h\nu, H) \propto |M^x_{\mathrm{TA}}|^2 \left( \beta(p) \int^{+\infty} k^2_x D^{e*}_{1/2} f(E^e_F) D^{h*}_{1/2+p} f(E^h_F)\, dE^e + \gamma(p) \int_{-\infty}^{+\infty} k^2_x D^{e*}_{-1/2} f(E^e_F) D^{h*}_{-1/2+p} f(E^h_F)\, dE^e \right) . \tag{17}$$

$E^h = h\nu - E^e - E'^{\mathrm{TA}}_g(H)$, $x$ denotes $e\perp$ or $h$, and a shortened form of notation has been used, as compared to Eq. (7). Rewriting the $k$ dependence of the transition probability as an energy dependence, we are able to derive effective densities of states for the TA recombination that include the reduced transition probabilities for carriers having small wave vectors, i.e., small energies (see Appendix B). These effective densities of states for electrons and holes are shown in Figs. 15 and 16 and should be compared to Figs. 3 and 4. In this way the numerical calculation for the line shape of the EHL (TA) band becomes equivalent to the calculation of the EHL (LA) band presented in Sec. III C, with the mere difference that now the effective density of states for the TA recombination are used. As a final step, the theoretical shape of the EHL (TA) line is computed for the two limiting cases in Eq. (16). In the first case, where we assume only the electron contribution to be present, the effective density of states of the electrons is convoluted with the actual density of states of the holes, and vice versa for the second case. We have not attempted an independent determination of the parameters $\Gamma_0$, $\xi$, and $n$ but have taken them from the EHL (LA) results. The chemical potential $\mu^{\mathrm{TA}}(H)$ is also deduced from $\mu^{\mathrm{LA}}(H)$ by adding the energy difference between the LA and TA phonon (19.7 meV).[63] Thus, the fit to the EHL (TA) lineshape is completely determined by the EHL (LA) results. Our only option is the choice of the form of the matrix element (16) to be decided by the experimental result. For comparison with the unpolarized measured spectra, the line shapes are calculated for all possible polarizations and then summed, with account taken of their relative contributions, to obtain the total intensity.

Figure 17 presents the theoretical results in comparison with the experimental data for four different flux densities. In all cases, the EHL (TA) line shape synthesized using only the hole term in the electron-phonon matrix element expansion agrees well with the experiment, while the complementary theoretical curve (electron

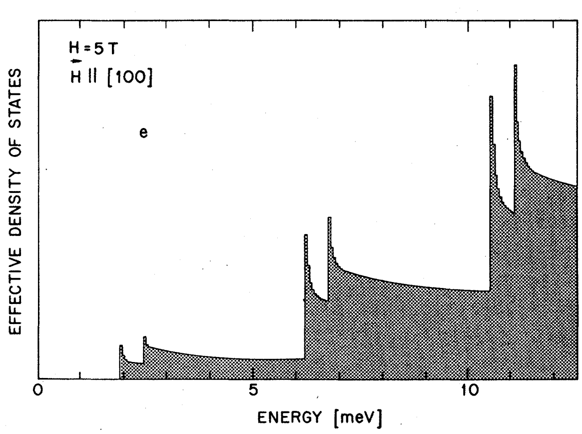


FIG. 15. Effective density of states of the electrons for the calculation of the EHL (TA) luminescence line.

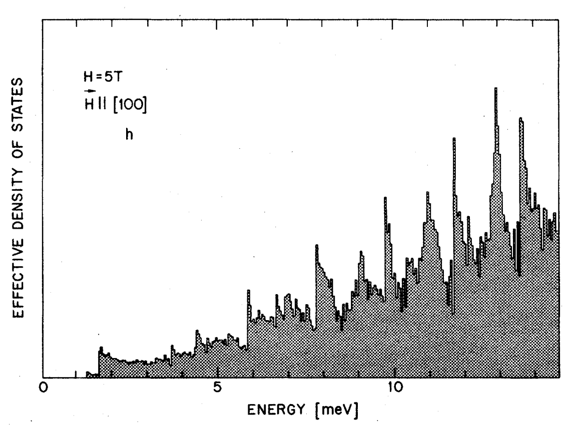


FIG. 16. Effective density of states of the holes for the calculation of the EHL (TA) luminescence line.

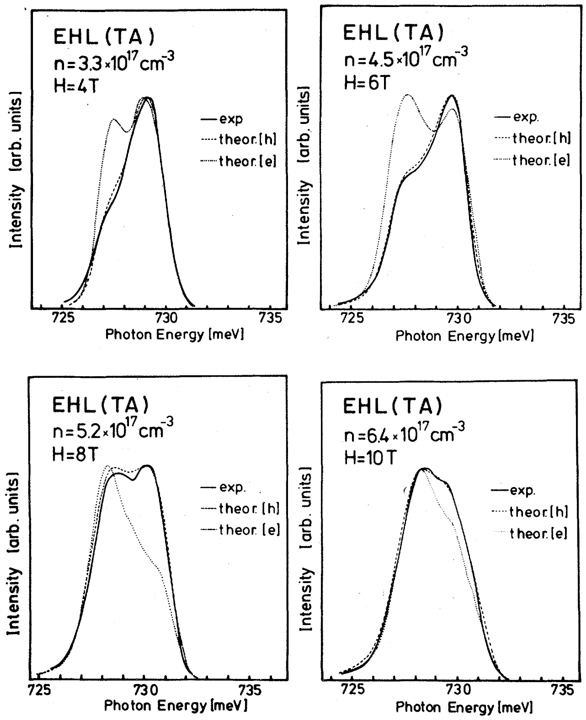


FIG. 17. Comparison of experimental and theoretical EHL (TA) line shapes for various flux densities. Voigt configuration, unpolarized: Dashed line ---- represents $|M^h_{\rm TA}|^2|k_h|^2 \gg |M^e_{\rm TA}|^2|k_e|^2$, dotted line ···· represents $|M^e_{\rm TA}|^2|k_e|^2 \gg |M^h_{\rm TA}|^2|k_h|^2$.

term only) deviates strongly. This result establishes even more emphatically than the zero-field analysis of the EHL (TA) line[61] that the main contribution to the EHL (TA) line comes from the hole term in the expansion of the electron-phonon matrix element. We believe that this preference originates from the fact that the average $k_h^2$ is much larger than the average $k_{e\perp}^2$ due to the extremely slim ellipsoidal Fermi surfaces of the electrons. Incidentally, the good line fits we have just obtained can be regarded as another independent check of the accuracy of the parameters of the condensate found from the EHL (LA) analysis.

## VI. FIELD DEPENDENCE OF THE TOTAL INTENSITIES

Having discussed the structures on the luminescence line and their origin we shall now turn to the total intensities of the luminescence bands integrated over $h\nu$. In general, our experimental results on the field dependence of the total EHL (LA) intensity agree with the data of Betzler *et al.*[5,6] measured in fields up to 3 T. We differ from those authors regarding the relative intensity of the oscillations, which presumably results from differences in experimental conditions.[64] For higher magnetic fields a monotonic decrease of the total intensity in the Voigt configuration and a relatively constant total intensity in the Faraday configuration is observed, both with weak oscillations in the $e$-$h$ density (see also Sec. IV).

However, the total intensity varied somewhat from run to run although, we hasten to add, the luminescence line shape in all cases was reproducible. Because the position of the magneto oscillations did not change we believe that this effect is due to a field dependence of the shape of the electron-hole droplet cloud around the laser spot. A contraction (or elongation) of this cloud can lead to an increase (or decrease) of the total intensity that falls on the detector due to purely geometrical reasons and must not necessarily be related to a change of the quantum efficiency of the recombination process. However, measurements of the ratio of total intensities are not affected, e.g., the ratio of the total EHL (TA) luminescence $I_{\rm TA}$ compared to the total EHL (LA) luminescence $I_{\rm LA}$. The field dependence of $I_{\rm TA}(H)/I_{\rm LA}(H)$ will provide an independent check for the results of Sec. V B on the nature of the TA-assisted radiative recombination mechanism and will be outlined below. The other important ratios of total intensities are $I_{\sigma+}/I_{\sigma-}$ in Faraday and $I_\sigma/I_\pi$ in Voigt configuration. They could provide a very sensitive source for the determination of the field dependence of the $e$-$h$ density. Unfortunately our data on these polarization ratios are too incomplete to report at the present time.

### A. Experimental results on the ratio $I_{TA}(H)/I_{LA}(H)$

The relative intensities of the TA and LA line were determined in two steps. First the total intensities of both lines were evaluated at various field strengths by graphically integrating the TA and LA luminescence of complete spectra taken at fixed magnetic fields (no polarizers were used because of the weak intensity of the TA signals). This procedure has the advantage over previously used methods[5,6] (that recorded the total intensity directly by using a monochromator with widely opened slits as a band filter) of being free from any falsification of the result caused by the energetic boundaries and the transmission characteristics of the filter used (e.g., slit function of the monochromator). Figure 18 shows the result of that procedure. At $H=0$, the total intensity of the *EHL* (TA) line is about 6% that of the *EHL* (LA) intensity. With increasing $H$ this ratio stays approximately constant until about 2.5 T, then it increases and follows an almost linear law for fields higher than about 4 T.

We explain this behavior as follows: For $H$

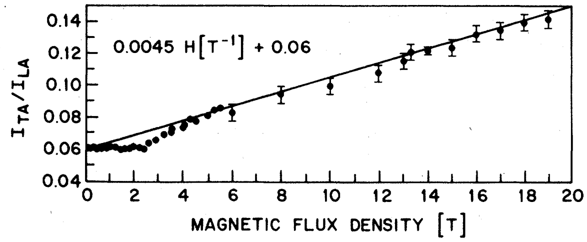


FIG. 18. Dependence of the relative intensities $I_{TA}/I_{LA}$ upon magnetic field. The slope of the line, drawn to describe the high-field region, agrees with the result of our calculations.

small, when the separation between Landau levels is small compared to the Fermi energies, the changes of the $k$ vectors due to the rearrangement of the states in $k$ space is small compared to the Fermi vectors, i.e., the Fermi surfaces are essentially unperturbed. Thus the $k$-dependent TA recombination process is unaffected. For high fields, when the Landau quantization becomes dominant (starting approximately at 2.5 T the electronic system is in the quantum limit) there is an increase of the EHL (TA) luminescence because of the expansion of the Fermi surface. This is shown explicitly in the calculations that follow.

### B. Calculation of the ratio $I_{TA}(H)/I_{LA}(H)$

#### *1. In the absence of a magnetic field*

We begin by deriving an expression for the ratio of the EHL (LA) and EHL (TA) luminescence intensities in the absence of field. Our approach is similar to that of Bénoît à la Guillaume *et al.*[57] and of Martin.[61] The total intensity of the EHL (LA) luminescence $I_{LA}(H=0)$ is the integral of Eq. (3) over $h\nu$ which gives

$$I_{LA}(0) \propto |M_{LA}|^2 n(0)^2 . \tag{18}$$

A similar integral gives the EHL (TA) total intensity (see Appendix C)

$$I_{TA}(H=0) \propto 5.39 |M^h_{TA}|^2 n(0)^{8/3} , \tag{19}$$

which leads to the ratio,

$$\frac{I_{TA}}{I_{LA}}(H=0) = 5.39 C \frac{|M^h_{TA}|^2}{|M_{LA}|^2} n(0)^{2/3} , \tag{20}$$

where $C$ is a constant assumed to be field independent. Using our experimental values $n(0) = 2.55 \times 10^{17}$ cm$^{-3}$ and $(I_{TA}/I_{LA})_{H=0} = 0.061$, we obtain a value for the ratio of squares of the matrix elements which we need in calculations to follow:

$$C \frac{|M^h_{TA}|^2}{|M_{LA}|^2} = 2.94 \times 10^{-14} \text{ cm}^2 . \tag{21}$$

#### *2. In the presence of a magnetic field*

The total intensity of the EHL (LA) luminescence in a magnetic field is evaluated in complete analogy to the zero-field case by integration of Eq. (7) with respect to the photon energy $h\nu$ and summation over all polarizations $p$. This leads to

$$I_{LA} \propto |M_{LA}|^2 n'(H)^2 , \tag{22}$$

$$n'(H)^2 = n^e_{1/2}(H) \sum_p \beta(p) n^h_{1/2+p}(H) + n^e_{-1/2}(H) \sum_p \gamma(p) n_{1/2+p} . \tag{23}$$

[$\beta(p)$ and $\gamma(p)$ are defined in Sec. III B.] The partial densities of the band are defined by

$$n^x_i(H) = \int_0^{E^x_F} D^x_i(E^x) dE^x , \quad x = e, h , \tag{24}$$

where the magnetic quantum numbers take the values $i = \pm\frac{1}{2}, \pm\frac{3}{2}$ for the holes and $i = \pm\frac{1}{2}$ for the electrons. The total intensity of the EHL (TA) luminescence cannot be reduced to an expression as simple as in the case of EHL (LA). Setting $x = h$, the integration of Eq. (17) with respect to $h\nu$ and summation over all polarizations results in[65]

$$I_{TA}(H) \propto |M^h_{TA}|^2 \left( n^e_{1/2}(H) \sum_p \beta(p) \int_0^{E^h_F} (k^2_\perp + k^2_H) D^h_{1/2+p} dE^h + n^e_{-1/2}(H) \sum_p \gamma(p) \int_0^{E^h_F} (k^2_\perp + k^2_H) D^h_{-1/2+p} dE^h \right) , \tag{25}$$

where we used the substitution $k^2_h = k^2_\perp + k^2_H$ developed in Appendix B.

In principle the integrals of Eq. (25) can be evaluated numerically to yield the field dependence of the ratio $I_{TA}/I_{LA}$. However, the important physical features are clearer if we make an approximation: From the line-shape analysis of Sec. III C we know that in fields higher than 8 T only the four lowest Landau levels of the valence band are populated. An inspection of these eigenstates shows that they all consist mainly of envelope functions with Landau quantum number $n = 0$, with admixture of higher $n$'s of less than 4%. Hence under these circumstances, $k^2_\perp$ of Eq. (25) is almost energy independent and equal to $(e/\hbar c)H$ (see Appendix B), resulting in an enormous simplification:

$$I_{\mathrm{TA}}(H) \propto |M_{\mathrm{TA}}^h|^2 n'(H)\left(\frac{e}{\hbar c}H + \langle k_H^2\rangle\right). \tag{26}$$

The $k_H$ dependence is included in $\langle k_H^2\rangle$ which stands for the squares of the wave vectors parallel to the field, averaged over all hole states:

$$\langle k_H^2\rangle = \frac{1}{n'(H)^2}\left(n_{1/2}^e(H)\sum_p \beta(p)\int_0^{E_F^h} k_H^2 D_{1/2+p}^h\, dE^h + n_{-1/2}^e(H)\sum_p \gamma(p)\int_0^{E_F^h} k_H^2 D_{-1/2+p}^h\, dE^h\right). \tag{27}$$

The ratio of the total intensities follows immediately:

$$\frac{I_{\mathrm{TA}}(H)}{I_{\mathrm{LA}}(H)} = C\frac{|M_{\mathrm{TA}}|^2}{|M_{\mathrm{LA}}|^2}\left(\frac{e}{\hbar c}H + \langle k_H^2\rangle\right), \tag{28}$$

where $C$ is the same constant as in Eq. (20). This reduces to

$$\frac{I_{\mathrm{TA}}(H)}{I_{\mathrm{LA}}(H)} = \alpha H + \eta,$$

$$\alpha = 4.50\times 10^{-3}\ (\mathrm{T}^{-1}),\quad \eta = 2.96\times 10^{-14}\langle k_H^2\rangle\ (\mathrm{cm}^2) \tag{29}$$

with the help of Eq. (21). The first term, linear in $H$, reproduces exactly the slope of the experimental results for fields higher than 4 T (see Fig. 18). This finding suggests that the increase of the intensity of the EHL (TA) line is a result of the expansion of the hole wave functions in $k$ space *perpendicular* to the field direction.

The second term, $\eta$, then has to be field independent. We did not perform the detailed numerical calculations necessary to evaluate $\langle k_H^2\rangle$ via Eq. (27) but demonstrate in Appendix D that, making some simplifying assumptions about the bands and the $e$-$h$ density, $\langle k_H^2\rangle$ actually turns out to be field independent, leading to a value of 0.038 for $\eta$. This value is 35% smaller than the experimental result 0.061 in Fig. 18. However, considering the simplifications in the evaluation of $\langle k_H^2\rangle$, this agreement is satisfying.

In summary, we can state that the increase of the total intensity of the EHL (TA) recombination under the influence of a magnetic field can be understood on the basis of a linear dependence of the TA electron-phonon matrix element on the wave vector of the holes involved in the recombination process outlined in Sec. V B.

## VII. CONCLUSION

In conclusion we have reported the first data on the optical recombination spectra of the $e$-$h$ liquid in Ge in very high magnetic fields (up to 19 T) including the LA-, TO-, and TA-assisted recombination lines and the complete polarization properties of the strongest, the EHL (LA) line.

In an analogy to the zero-field case, all experimental data on the shape of the EHL (LA) line in all four polarizations can be fitted theoretically by convoluting the one-particle densities of states around the extrema of valence and conduction bands of Ge in the presence of a magnetic field. The structure in the recombination line is a result of singularities appearing in the densities of states of the bands due to Landau quantization. A discrepancy in the width between experimental and theoretical line shapes can only be resolved if we invoke a mass renormalization of the carriers of approximately 10%. Extrapolating to zero field we conclude that a renormalization of the same magnitude also exists in the absence of a magnetic field.

Our fitting procedure yields accurate data on the field dependence of the following EHL parameters:

(1) ground-state energy,
(2) electron-hole density, and
(3) work function.

In going to the highest fields we find a continuous increase of the ground-state energy by more than a factor of 2, an increase of the electron-hole density by more than a factor of 4, an almost field-independent work function, and a decrease of the quasiparticle lifetime by approximately a factor of 2. The behavior of ground-state energy and $e$-$h$ density can be understood as resulting from the field-induced increase of the densities of states at the bottom of the bands.

Our theoretical calculation, based on the assumption that the sum of exchange and correlation energies is only density but not directly field dependent, is in good agreement with the experimental data over a large field range. This calculation also reproduces the small oscillations in the $e$-$h$ density that are responsible for most of the magneto-oscillatory effects reported earlier. All EHL parameters show a continuous variation with magnetic field. From this fact we conclude that no additional phase transition occurs in the electron-hole liquid under the influence of a magnetic field.

Our experiments elucidate the nature of the electron (hole)–phonon interaction essential to the recombination process. First, they show (even more strongly than in the zero-field work) the EHL (TA) line shape can be generated theoretically if we assume that the interaction matrix element is linearly dependent on the carrier wave vector, specifically the wave vector of the *holes*. Second, measurements of the integrated intensity of the EHL (TA) line with respect to the EHL (LA) line reveal an increase of a factor of 2 when we go to our highest fields, a result which can be understood quantitatively in terms of the form of the recombination matrix element quoted above.

From a theoretical point of view the quantum limit, a situation where all carriers condense into the $n=0$ Landau level, represents a most interesting configuration. Our experiments, however, reveal that for the EHL in Ge the quantum limit cannot be reached in fields of 19 T. Though the electronic system reaches this limit at approximately 2 T, four Landau levels of the valence band remain populated up to 19 T and the picture is greatly complicated by the strong nonparabolicities (camelbacks) of the hole dispersion. This makes accurate theoretical calculations on the ground-state parameters impractical. The quantum limit, however, simplifies this situation considerably. There exist various theories that apply for this case that bear interesting analogies to degenerate proton-electron systems in ultrahigh magnetic fields (up to $10^8$ T) as they might exist in the universe. The realization of a model system of an EHL in the quantum limit therefore is highly desirable. The application of sufficiently high fields to the EHL in Ge seems not to be practical in the near future. Assuming that the Fermi energy stays constant, an assumption that holds reasonably well up to 19 T at least in the [100] direction, fields of approximately 200 T are necessary to reach the quantum limit in the valence band. The study of other substances that show condensation also seems not to solve the problem. They all exhibit degenerate bands that will result in similar complicated dispersion relations in a magnetic field, but only in Ge has the valence band in a magnetic field been studied extensively.

A way to reach the quantum limit for the EHL might be to apply stress to the semiconductor under study. The inspection of two graphs given in Ref. 17 showing the energetic shifts of the valence bands of Ge under the influence of simultaneous stress and magnetic field reveals that for the [100] direction as well as for the [111] direction the lowest two levels ($n=0$, spin $\pm\frac{1}{2}$, in the limit of very high field strength) can be split apart from the remaining levels by 10 to 15 meV in fields of 20 T and stresses of $10^4$ kg/cm$^2$. Both values are technically attainable. A combination of high stress and high magnetic field might be able to produce a situation where existing many-particle theories for the quantum limit can be checked for the first time and the predicted electron-hole fibers (EHF) might occur. To reach the *extreme* quantum limit, however, a configuration where only the lowest spin states of the $n=0$ Landau levels are populated, fields higher than 20 T are needed. This limitation is due to the small spin splitting of the electrons. Under the assumption of a constant Fermi energy, fields higher than 22 T in the [111] direction and higher than 25 T in the [100] direction would be necessary to reach the extreme quantum limit for the electrons. However, the assumption of a constant Fermi level might be too pessimistic as it is known to decrease when uniaxial stress is applied to the sample.[72]

## ACKNOWLEDGMENTS

We would like to thank H. J. Queisser, M. H. Pilkuhn, and K. Dransfeld for continuous interest in this work, and H. J. Q. and M. H. P. for carefully reading the manuscript. We are indebted to J. C. Hensel for making available to us his unpublished results on the valence-band dispersion and assistance during the numerical calculations, for carefully reading the manuscript, and for many valuable suggestions. Our thanks go to R. Ranvand for the calculation of the nonlinearities in the field dependence of the Landau ladder and many interesting conversations, to R. Conradt for pointing out the applicability of Landsberg's theory to the broadening of the EHL line, to A. P. J. van Deursen and J. F. Koch for assistance in the cyclotron measurements, and to L. M. Sander for the valuable suggestion for the calculation of the field dependence of the ground-state energy. We also would like to thank T. M. Rice for helpful comments on the manuscript. Finally, we would like to thank the staff of the SNCI-HML Grenoble for support during the experiments. The work was in part supported by the Deutsche Forschungsgemeinschaft in the framework of SFB 67.

## APPENDIX A: CALCULATION OF THE FIELD DEPENDENCE OF THE GROUND STATE

In zero magnetic field, the ground-state energy per $e$-$h$ pair $E_G$ and the equilibrium density $n_0$ is determined by the minimum of the sum of three contributions: the kinetic energy $E_{\text{kin}}$, the exchange energy $E_x$, and the correlation energy $E_c$[66]:

$$E_G = \min[E_{\text{kin}}(r_s) + E_{xc}(r_s)], \tag{A1}$$

where we combined $E_{xc} = E_x + E_c$.

Both terms depend only upon the interparticle spacing $r_s$ being proportional to $n^{-1/3}$ ($n$ represents the $e$-$h$ density). $E_G$ is measured relative to the band-gap $E_g$. Analytic expressions exist for $E_{\text{kin}}$ and $E_x$ while the term $E_c$ is calculated numerically and tabulated. The values of $E_c$ ($r_s$) depend on the underlying theoretical concept. However, the ground-state parameters calculated with various tabulated correlation energies given in the literature[67-70] altogether show good agreement with experiment.[1]

To calculate the ground-state parameters of the EHL in a magnetic field $H$, we proceed in the same way as in the absence of a magnetic field. The ground-state energy at equilibrium is found by minimizing with respect to $r_s$:

$$E_G(H) = \min[E_{\mathrm{kin}}(r_s, H) + E_{xc}(r_s, H)]. \qquad \text{(A2)}$$

Under the assumption that $E_{xc}$ is only density but not explicitly field dependent, expression (A2) simplifies to

$$E_G(H) \approx \min[E_{\mathrm{kin}}(r_s, H) + E_{xc}(r_s, 0)]. \qquad \text{(A3)}$$

To smooth out the singularities occurring in the numerical calculations and for a better match with the experimental condition, we actually calculate the free energy $F_G(r_s, H, T)$ at a temperature of 2.5 K and minimize it with respect to $r_s$. Again we neglect the temperature dependence of $E_{xc}$ which was shown to be small.[71] In this way we yield for the average energy $E$ per $e$-$h$ pair

$$E(H, T) \approx \min[E_{\mathrm{kin}}(r_s, H, T) + E_{xc}(r_s, 0, 0)]. \qquad \text{(A4)}$$

However, for the purpose of comparing theory with experiment we will not distinguish between $E_G(H)$ and $E(H, T = 2.5\text{ K})$. The difference between both values is of the order of $\frac{1}{20} E_G(H)$,[71] which is comparable with the experimental accuracy. The average kinetic energy per electron-hole pair $E_{\mathrm{kin}}(r_s, H, T)$ can simply be calculated numerically on the basis of the density of states in a magnetic field $D^e(E^e, H)$ and $D^h(E^h, H)$ developed in Sec. III C:

$$E_{\mathrm{kin}}(r_s, H, T) = \frac{\int_0^\infty D^e(E^e, H) f(E^e, E_F^e(r_s H), T) E^e dE^e}{n(r_s, H)} + \frac{\int_0^\infty D^h(E_h, H) f(E^h, E_F^h(r_s, H), T) E^h dE^h}{n(r_s, H)}. \qquad \text{(A5)}$$

The Fermi energies $E_F^e(r_s, H)$ and $E_F^h(r_s, H)$ were evaluated iteratively using the equations

$$n(r_s, H) = \int_0^\infty D^e(E^e, H) f(E^e, E_F^e(r_s, H), T) dE^e = \int_0^\infty D^h(E^h, H) f(E^h, E_F^h(r_s, H), T) dE^h. \qquad \text{(A6)}$$

The exchange energy expressed in units of the theoretical exciton Ry[70] is

$$E_x(r_s, 0) = -\frac{1.1503}{r_s}. \qquad \text{(A7)}$$

For the correlation energy we use two tabulated functions of Ref. 69 (SPH II is a self-consistent particle-hole approximation, HA II is a Hubbart approximation) which in conjunction with $E_{\mathrm{kin}}$ and $E_x$ describe well the experimental ground-state parameters in zero field. The tabulated values of the two functions were approximated by the interpolation formula $E_c(r_s) = A + B/\sqrt{r_s}$. The constants $A$ and $B$ were determined empirically to ensure an optimum agreement in the range $0.2 \le r_s \le 1$.

The results are summarized in Fig. 19 which reproduces a set of curves of the free energy per $e$-$h$ pair relative to the band-edge energy $E_g(H = 0)$ as a function of the mean pair distance $r_s$ in the field range from 0 to 20 T. The ground-state energy $E_G(H)$ and the equilibrium density $n_0(H)$ can directly be extracted from the minima of the set. With increasing magnetic field, the minima shift to smaller values of $r_s$ and therefore to higher densities, an observation which meets the experimental results. The precise numerical determination of the minima in small steps of 0.1 T yields a magnetic-field dependence of the equilibrium density and ground-state free energy shown in Figs. 11 and 12. They are discussed in Sec. IV.

## APPENDIX B: EFFECTIVE DENSITIES OF STATES FOR THE TA-ASSISTED RECOMBINATION

Equation (17) for the TA line shape is equivalent to Eq. (7) for the LA line shape except for the inclusion of the quantity $k_x^2$ ($x$ being $h$ or $e_\perp$). In this

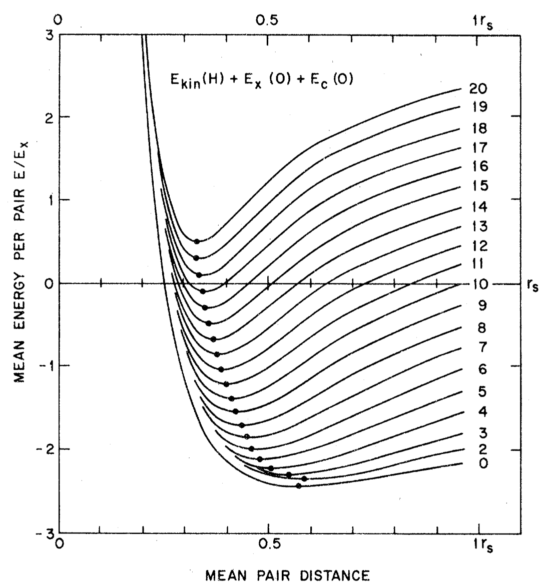


FIG. 19. Total energy per $e$-$h$ pair as a function of the mean distance between pairs at various magnetic-flux densities. The numbers on the curves denote the flux density in T. The energy is expressed in units of the exciton Ry and measured relative to the band edge at zero-field $E_g(H = 0)$. The distance between pairs is expressed in units of the exciton Bohr radius.

appendix we show how this term can be combined with the related density of states ($D^e_{S_i}$ or $D^h_{M_j}$) to obtain an effective density of states for the TA recombination, which then can be used in the standard way for line-shape calculations.

First we transform the $k$ dependence into an energy dependence. We use the following qualitative picture: The eigenenergies $E_h(k_H)$ of an isotropic parabolic band with an effective mass $m^*$ in a magnetic field $H$ are given by

$$E_h(k_H) = (n+\tfrac{1}{2})\hbar\omega_c + \frac{\hbar k_H^2}{2m^*}, \; n = 0,1,2,\ldots \tag{B1}$$

where $\omega_c = eH/m^*c$ is the cyclotron frequency, $k_H$ the component of the wave vector parallel to $H$, and $n$ the Landau quantum number. The eigenstates are restricted to rotational cylinders centered around the field axis. The quantization in the direction of $H$ remains unchanged. We can define

$$k_\perp^2 = (2n+1)\frac{eH}{\hbar c}, \tag{B2}$$

which is a measure of the momentum of the particle in the plane perpendicular to the field and yields for the total wave vector

$$k^2 = k_\perp^2 + k_H^2 . \tag{B3}$$

For the strongly anisotropic situation of electrons and holes in Ge this simple model does not directly apply and we have to work in an approximate scheme.

### A. Electrons, $\vec{H} \parallel [0001]$

We work out, in a semiclassical way, the surfaces in $k$ space that represent the eigenstates of the electrons for $\vec{H} \parallel [001]$, the direction of field used in our experiments. We find that these surfaces are concentric tubes centered around an axis that is only slightly (4.2°) inclined with respect to the axis of the electron Fermi surface, i.e., the $\Lambda$ axis, (see Fig. 20). In fields higher than ~2.5 T only the innermost of these cylinders is populated and expands with increasing field. Figure 20 shows for an arbitrary electronic state on this cylinder its wave vector $\vec{k}_\perp$ defined in Eq. (B3) as well as $\vec{k}_{e\perp}$, the quantity that determines via Eq. 16 the strength of the phonon coupling in case of the TA transition. As an approximation to $k_{e\perp}$, the distance of the state from the $\Lambda$ line, which actually depends slightly on $k_H$, we use $k_{e\perp}^2 \approx k_0^2 = k_\perp^2 \sin^2\alpha$. The constant sin term can be neglected, because our line-shape calculation yields only relative and no absolute values. Using relation (B2) we finally obtain

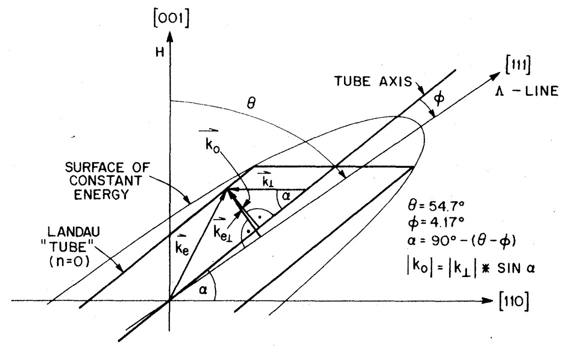


FIG. 20. Evaluation of the wave vector that is relevant for the TA-assisted radiative recombination.

$$k_{e\perp}^2 \approx (2n+1)\frac{eH}{\hbar c}. \tag{B4}$$

This is combined with the electron densities $D^e_{\pm 1/2}$ from (8) to result in the effective densities of states for the TA recombination shown in Fig. 15:

$$k_{e\perp}^2 D^e_{\pm 1/2}(E^e, H) \approx m_z^* H^2 \sum_n (2n+1) \times \left[E^e - \left(\frac{2n+1}{m_c^*/m_0} \pm \frac{g}{2}\right)\mu_B H\right]^{-1/2} \tag{B5}$$

(constants of proportionality have been omitted).

### B. Holes

For the purpose of the evaluation of $k_h^2$ of Eq. (16), an isotropic model is a reasonably good approximation to the valence band of Ge, so that expression (B3) can be used. The effective densities of states for the TA process, however, can only be calculated numerically. For each hole state [see Eq. (10)]

$$\phi_m(k_H) = \sum_n \sum_{M_j} a_n(k_H, M_j) u_n |k_H, M_j\rangle, \tag{B6}$$

the value for $k_h^2$ as defined in Eq. (B2) is a sum of an average $k_\perp^2$, perpendicular to the field, calculated via Eq. (B2) and the square of the explicitly appearing wave vector parallel to the field $k_H$:

$$k_h^2(\phi_m(k_H)) = \sum_{n,M_j} \left(|a_n(k_H, M_j)|^2 (2n+1)\frac{eH}{\hbar c}\right) + k_H^2 . \tag{B7}$$

Then, for the effective density of states, each eigenstate $\phi_m(k_H)$ having energy $E_m(k_H)$ is not counted with the weight 1 as in the LA case, but with the weight $k_h^2(\phi_m(k_H))$. The distribution over the various magnetic quantum numbers $M_j$ is performed, as in the LA case, via Eq. (11). This yields four weighted density of states $k_h^2 D^h_{M_j}(E^h, H)$, the sum of which is shown in Fig. 16 for a flux density of 5 T.

## APPENDIX C: TOTAL INTENSITY OF THE EHL(TA) LUMINESCENCE IN ZERO FIELD

The total luminescence intensity for the EHL is the integral of Eq. (3) over $h\nu$. In treating the TA line we substitute in the integral the approximate form of the square of the recombination matrix element $|M_{\mathrm{TA}}(\vec{k}_e, \vec{k}_h)|^2 \approx |M_{\mathrm{TA}}^h|^2 k_h^2$ established in Sec. V B and obtain for $T=0$ the following:

$$I_{\mathrm{TA}}(H=0) \propto |M_{\mathrm{TA}}^h|^2 \times \int_{E_g^{\prime}\mathrm{LA}}^{E_g^{\prime}\mathrm{LA}+E_F} \left( \int_0^{E_F^e} D_e(E^e) k_h^2 D_h(E^h)\, dE^e \right) dh \,, \tag{C1}$$

where $E_F = E_F^e + E_F^h$ and

$$E^h = h\nu - E^e - E_g^{\prime \mathrm{LA}} \,. \tag{C2}$$

We transform the integration over $h\nu$ into an integration over $E_h$ using relation (C2) and perform the integration over $E^e$. Noticing that $\int_0^{E_F^e} D_e(E^e) dE^e = n(0)$ and that $D_h(E^h)=0$ for $E^h<0$, Eq. (C1) results in

$$I_{\mathrm{TA}}(0) \propto |M_{\mathrm{TA}}^h|^2 n(0) \int_0^{E_F^h} k_h^2 D_h(E^h)\, dE^h \,. \tag{C3}$$

Moreover, we assume that $|M_{\mathrm{TA}}^h|^2$ is equal for light (lh) and heavy (hh) holes. Assuming isotropic bands and with the help of the usual relationships

$$k_{\mathrm{hh}}^2 = \frac{2m_{\mathrm{hh}}}{\hbar^2} E^h \text{ and } k_{\mathrm{lh}}^2 = \frac{2m_{\mathrm{lh}}}{\hbar^2} E^h \,,$$

we write the total intensity as

$$I_{\mathrm{TA}}(0) \propto |M_{\mathrm{TA}}^h|^2 n(0) \left( \frac{2m_{\mathrm{hh}}}{\hbar^2} \int_0^{E_F^h} E D_{\mathrm{hh}}(E^h)\, dE^h + \frac{2m_{\mathrm{lh}}}{\hbar^2} \int_0^{E_F^h} E D_{\mathrm{lh}}(E^h)\, dE^h \right) \tag{C4}$$

in terms of the density of states for light ($D_{\mathrm{lh}}$) and heavy ($D_{\mathrm{hh}}$) holes, respectively. This yields upon integration

$$I_{\mathrm{TA}}(0) \propto |M_{\mathrm{TA}}^h|^2 [n(0)]^{8/3} \tfrac{3}{5} (3\pi^2)^{2/3} + \frac{1 + \left( \frac{m_{\mathrm{lh}}}{m_{\mathrm{hh}}} \right)^{5/2}}{\left[ 1 + \left( \frac{m_{\mathrm{lh}}}{m_{\mathrm{hh}}} \right)^{3/2} \right]^{5/3}} \tag{C5}$$

Owing to the large difference between light and heavy hole masses ($m_{\mathrm{lh}}/m_{\mathrm{hh}} = 0.121$)[67] the last factor is close to unity. Inserting the appropriate numbers into Eq. (C5) eventually results in

$$I_{\mathrm{TA}}(0) \propto 5.39 |M_{\mathrm{TA}}^h|^2 [n(0)]^{8/3} \,. \tag{C6}$$

## APPENDIX D: $\langle k_H^2 \rangle$ FOR A DEGENERATE PARABOLIC BAND

We derive a simple expression based on a model band structure for the average of $k_H^2$ which finds application in Sec. VI B. For a $q$-fold degenerate, isotropic, and parabolic band of mass $m^*$ in a magnetic field $H$, the density of states for the lowest Landau level is given by

$$D(E) = qfE^{-1/2} \text{ with } f = \left( \frac{2m^*}{\hbar^2} \right)^{1/2} \frac{1}{4\pi^2} \frac{eH}{\hbar c} \tag{D1}$$

(the origin of the energy scale is at the bottom of the Landau level). Thus, the (field-dependent) Fermi energy at $T=0$ is

$$E_F(H) = \left( \frac{n(H)}{2qf} \right)^2 . \tag{D2}$$

If $k_H$ is the wave vector in the direction of the magnetic field, then the average $k_H^2$ can be expressed (at $T=0$) as,

$$\langle k_H^2 \rangle = \frac{1}{n(H)} \int_0^{E_F(H)} k_H^2 D(E)\, dE \,. \tag{D3}$$

Using equations (D1) and (D2) and $k_H^2 = 2m^* E/\hbar^2$ we obtain

$$\langle k_H^2 \rangle = \frac{4}{3} \frac{\pi^4}{q^2} \frac{n(H)^2}{H^2} \left( \frac{\hbar c}{e} \right)^2 . \tag{D4}$$

Assuming a proportionality between the carrier density and the field strength such as $n(H) = \rho H$, $\langle k_H^2 \rangle$ can be written as

$$\langle k_H^2 \rangle = \tfrac{4}{3} \pi^4 \frac{\rho^2}{q^2} \left( \frac{\hbar c}{e} \right)^2 . \tag{D5}$$

This result shows that for a linear field dependence of the carrier density, $\langle k_H^2 \rangle$ is independent of the effective mass and independent of the flux density.

For the $e$-$h$ condensate in Ge, a linear dependence of the carrier density upon the magnetic field is a good approximation for the region above 8 T. There the density varies as $n = \rho H$, with $\rho = 6 \times 10^{16}$ ($\mathrm{cm^{-3}\,T^{-1}}$), (see Fig. 12). With $q=4$, for the number of levels that are populated at fields above 8 T, $\langle k_H^2 \rangle$ turns out to be $\langle k_H^2 \rangle = 1.3 \times 10^{16}$ $\mathrm{cm^{-2}}$, which leads to the value 0.038 for the constant $\eta$ in Eq. (29).

*Present address: Bell Laboratories, 600 Mountain Avenue, Murray Hill, New Jersey 07974, USA.
†Present address: Fachhochschule für Technik, 73 Esslingen/N., FRG.

[1]For reviews see, e.g., Ya. E. Pokrovskii, Phys. Status Solidi A 11, 385 (1972); M. Voos and Bénoît à la Guillaume, in *Optical Properties of Solids*, edited by B. O. Seraphin (North-Holland, Amsterdam, 1975), p. 143; J. C. Hensel, T. G. Phillips, and G. A. Thomas, in *Solid State Physics*, edited by H. Ehrenreich, F. Seitz, and D. Turnbull (Academic, New York, 1978), Vol. 32; T. M. Rice, *ibid.*

[2]V. S. Bagaev, T. I. Galkina, N. A. Penin, V. B. Stopachinskii, and M. N. Churaeva, Pis'ma Zh. Eksp. Teor. Fiz. 16, 120 (1972) [JETP Lett. 16, 83 (1972)].

[3]A. F. Dite, V. G. Lysenko, V. D. Lokhnygin, and V. B. Timofeev, Pis'ma Zh. Eksp. Teor. Fiz. 18, 114 (1973) [JETP Lett. 18, 65 (1973)].

[4]V. N. Murzin, V. A. Zayats, and V. L. Kononenko, Fiz. Tverd. Tela. (Leningrad) 15, 3634 (1973) [Sov. Phys. Solid State 15, 2421 (1974)].

[5]K. Betzler, B. G. Zhurkin, and A. L. Karuzskii, Solid State Commun. 17, 577 (1975).

[6]K. Betzler, B. G. Zhurkin, A. L. Karuzskii, and B. M. Balter, J. Lumin. 12/13, 651 (1976).

[7]P. S. Gladkov, K. Betzler, B. G. Zhurkin, and A. L. Karuzskii, Zh. Eksp. Teor. Fiz. 69, 2199 (1975) [Sov. Phys.—JETP 42, 1118 (1976)].

[8]V. N. Murzin, V. A. Zayats, and V. L. Kononenko, in *Proceedings of the 11th International Conference on Semiconductors, Warsaw, 1972* (PWN-Polish Scientific, Warsaw, 1972), p. 678.

[9]K. Fujii and E. Otsuka, *Proceedings of the 12th European Congress on Molecular Spectroscopy, Strasbourg, 1975* (Elsevier, Amsterdam, 1976), p. 143.

[10]K. Muro and Y. Nisida, J. Phys. Soc. Jpn. 40, 1069 (1976).

[11]K. Fujii and E. Otsuka, J. Phys. Soc. Jpn. 38, 742 (1975).

[12]A. L. Karuzskii, K. W. Betzler, B. G. Zhurkin, and B. M. Balter, Pis'ma Zh. Eksp. Teor. Fiz. 22, 65 (1975) [JETP Lett. 22, 29 (1975)].

[13]A. K. Karuzskii, K. W. Betzler, B. G. Zhurkin, and B. M. Balter, Zh. Eksp. Teor. Fiz. 69, 1088 (1975) [Sov. Phys.—JETP 42, 554 (1976)].

[14]H. Büttner, in *Proceedings of the 12th International Conference on Semiconductors, Stuttgart, 1974*, edited by M. H. Pilkuhn (Teubner, Stuttgart, 1974), p. 81.

[15]S. T. Chui, Phys. Rev. B 9, 3438 (1974).

[16]J. C. Jones, P. R. Wallace, J. P. Ulmet, G. Carrere, and S. Askenazy, Phys. Status Solidi B 63, 201 (1974).

[17]K. Suzuki and J. C. Hensel (I), Phys. Rev. B 9, 4184 (1974); J. C. Hensel and K. Suzuki (II), *ibid.* 9, 4219 (1974); J. C. Hensel and K. Suzuki (III, IV), Phys. Rev. (to be published).

[18]V. S. Bagaev, T. I. Galkina, and O. V. Gogolin, in *Proceedings of the 10th International Conference on Semiconductors, Cambridge, Mass., 1970*, edited by S. P. Keller, J. C. Hensel, and F. Stern (U.S.A.E.C. Division of Technical Information, Springfield, Va., 1970), p. 500.

[19]A. S. Alekseev, V. S. Bagaev, T. I. Galkina, O. V. Gogolin, N. A. Penin, A. M. Semonov, and V. G. Stopachinskii, Pis'ma Zh. Eksp. Teor. Fiz. 12, 203 (1970) [JETP Lett. 12, 140 (1970)].

[20]V. M. Asnin, Yu. N. Lomasov, and A. A. Rogachev, Pis'ma Zh. Tekh. Fiz. 1, 596 (1975).

[21]V. M. Asnin, G. L. Bir, Yu. N. Lomasov, G. E. Pikus, and A. A. Rogachev, Fiz. Tverd. Tela (Leningrad) 18, 2011 (1976) [Sov. Phys. Solid State 18, 1170 (1976)].

[22]P. D. Altukhov, G. E. Pikus, and A. A. Rogachev, Pis'ma Zh. Eksp. Teor. Fiz. 25, 154 (1977) [JETP Lett. 25, 141 (1977)].

[23]P. D. Altukhov, V. M. Asnin, G. L. Bir, Yu. N. Lomasov, G. E. Pikus, and A. A. Rogachev, in *Proceedings of the 13th International Conference on Semiconductors, Rome, 1976*, edited by F. G. Fumi (Marves, Rome, 1976), p. 1094.

[24]R. W. Martin, H. L. Störmer, W. Rühle, and D. Bimberg, J. Lumin. 12/13, 645 (1976).

[25]H. L. Störmer, R. W. Martin, and J. C. Hensel, in *Proceedings of the 13th International Conference on Semiconductors, Rome, 1976*, edited by F. G. Fumi (North-Holland, Amsterdam, 1977), p. 350.

[26]In the meantime, more evidence for mass renormalization of the electrons appeared in magnetoplasma resonance experiments: V. I. Gavrilenko, V. L. Kononenko, T. S. Mandel'shtam, and V. N. Murzin, Pis'ma Zh. Eksp. Teor. Fiz. 23, 701 (1976) [JETP Lett. 23, 645 (1976)]. More recently even the angular dependence of the renormalization has been reported: V. I. Gavrilenko, V. L. Kononenko, T. S. Mandel'shtam, V. N. Murzin, and S. A. Saunin, Pis'ma Zh. Eksp. Teor. Fiz. 26, 102 (1977) [JETP Lett. 26, 96 (1977)].

[27]T. M. Rice, Nuovo Cimento 23B, 226 (1974).

[28]M. Rösler and R. Zimmermann, Phys. Status Solidi B 67, 525 (1975); T. M. Rice in Ref. 1.

[29]M. Lax and J. J. Hopfield, Phys. Rev. 124, 115 (1961).

[30]G. A. Thomas, E. I. Blount, and M. Capizzi, Phys. Rev. B 19, 702 (1979).

[31]H.-h. Chon, G. K. Wong, and B. J. Feldman, Phys. Rev. Lett. 39, 959 (1977).

[32]The spin-orbit splitting in Ge is large compared to all relevant hole energies of the condensate. Therefore, the holes are treated as spin-$\frac{3}{2}$ particles.

[33]L. M. Roth, B. Lax, and S. Zwerdling, Phys. Rev. 114, 90 (1959).

[34]L. M. Roth and P. N. Argyres, in *Semiconductors and Semimetals*, edited by R. K. Willardson and A. C. Beer (Academic, New York, 1966), Vol. 1, p. 159.

[35]See, e.g., B. Lax and J. G. Mavroides, *Solid State Physics*, edited by F. Seitz and D. Turnbull (Academic, New York, 1960), Vol. 11, p. 261.

[36]See, e.g., C. Kittel, *Introduction to Solid State Physics* (Wiley, New York, 1966).

[37]B. W. Levinger and D. R. Frankl, J. Phys. Chem. Solids 20, 281 (1961).

[38]G. Feher, D. K. Wilson, and E. A. Gere, Phys. Rev. Lett. 3, 25 (1959). In this paper we used the $g$ factor of the donor ground state in Ge, $g=\frac{1}{3}(2g_\perp+g_\parallel)$, $g_\perp$ and $g_\parallel$ being the $g$ factors perpendicular and parallel to $\Lambda$ line. In fact we should have used the value $g=(g_\parallel^2\cos^2\Theta+g_\perp\sin^2\Theta)^{1/2}=1.66$ with $\Theta$ being the angle between the [111] and field direction. However, in our line shape analysis at one stage we studied the influence of a varying $g$ factor on the line shape. We did not find any significant change for the range $1.5<g<1.7$. This can readily be understood, taking into account the effect of the lifetime broadening onto the density of states illustrated in Fig. 6. Therefore, our results will not be

affected by this oversight. We like to thank J. C. Hensel for bringing this point to our attention.

[39]J. M. Luttinger and W. Kohn, Phys. Rev. 97, 869 (1955); J. M. Luttinger, *ibid.* 102, 1030 (1956).

[40]R. L. Aggarwal, in *Semiconductors and Semimetals*, edited by R. K. Willardson and A. C. Beer (Academic, New York, 1972), Vol. 9, p. 222.

[41]C. R. Pidgeon and R. N. Brown, Phys. Rev. 148, 575 (1966).

[42]Recent cyclotron resonance measurements in the THz range on optically pumped Ge at low temperatures in magnetic fields up to 19 T confirmed these theoretical results: within 2% the cyclotron resonances of the holes scaled with those measured in the GHz range (Ref. 17) [H. L. Störmer, A. P. J. van Deursen, and J. F. Koch (unpublished)].

[43]P. T. Landsberg, Proc. Phys. Soc. London A62, 806 (1949).

[44]P. T. Landsberg, Phys. Status Solidi 15, 623 (1966).

[45]R. W. Martin and H. L. Störmer, Solid State Commun. 22, 523 (1977). The formalism of Landsberg has been applied successfully to the EHL (TA) and EHL (TO-LO) spectra in the case of silicon. W. Schmid, Ph.D. thesis, University of Stuttgart (unpublished).

[46]The electron temperature from the line-shape analysis $T \approx 2.5$ K was found to be always slightly above the bath temperature $T_b \approx 2$ K.

[47]Notice that the line shape is essentially a reproduction of the density of states of the holes. This results from the sharp peak of the electron distribution that is, convoluted with the hole density of states.

[48]The increase in density of Fig. 7(d) with respect to Fig. 7(b) results from the fact that the mass parallel to the $H$ field must be assumed to increase also by 10%.

[49]In fact, a slight tendency to higher values of $\xi$ seems to occur with increasing field, which presumably results from the field induced increase of the $e$-$h$ density.

[50]See the discussion in Ref. 24 of the 1975 International Conference on Luminescence.

[51]Strictly speaking, the work function $\Phi$ is determined by the difference between the bottom of the FE line and the chemical potential $\mu$. No information about the bottom of the FE line is available as we did not analyze the FE line shape in magnetic fields. However, the peak of the FE line is situated only a few tenths of a meV above the low-energy onset of the line. Hence, the distance between the FE (LA) and the $\mu^{\mathrm{LA}}$ points is very close to (slightly larger than) the work function $\Phi$. For zero-field free-exciton line-shape analysis see G. A. Thomas, A. Frova, J. C. Hensel, R. E. Miller, and P. A. Lee, Phys. Rev. B 13, 1692 (1976).

[52]In the meantime a change of carrier density was also reported for fields parallel to the [111] direction, where the degeneracy of the four electron valleys is lifted. V. L. Kononenko and V. N. Murzin, Pis'ma Zh. Eksp. Teor. Fiz. 24, 590 (1976) [JETP Lett. 24, 549 (1976)].

[53]The apparent disagreement between $\lim_{H\to 0} \Gamma_0(H)$ of Fig. 13 and $\Gamma_0(h=0)$ of Ref. 45 results from the difference in the energy dependence of $\Gamma(E)$ used in both cases.

[54]A temperature dependence of the parameter is neglected. The deviations of these parameter at an electron temperature of $T \approx 2.5$ K from those at $T = 0$ is smaller than 0.1 meV for $\mu$ and $\approx 0.2$ meV for $E_F$ and therefore smaller than the uncertainty of our data. The parameter $\Gamma$ has mainly the function to smooth the structures of the theoretically generated line but does not affect the position of the structures [G. A. Thomas, T. G. Phillips, T. M. Rice, and J. C. Hensel, Phys. Rev. Lett. 31, 386 (1973)].

[55]L. V. Keldysh and T. A. Onishchenko, Pis'ma Zh. Eksp. Teor. Fiz. 24, 70 (1976) [JETP Lett. 24, 59 (1976)].

[56]L. V. Keldysh and A. P. Silin, Fiz. Tverd. Tela (Leningrad) 15, 1532 (1973) [Sov. Phys. Solid State 15, 1027 (1973)].

[57]H. L. Störmer, Verh. Dtsh. Phys. Ges. 12, 102 (1977).

[58]In fact, most of the oscillatory effects are interpreted in terms of a slight $e$-$h$ density variation, periodic in $1/H$. However, the average density over the field range employed is supposed to be practically constant.

[59]We believe that the good agreement between experimental data and theoretical prediction of Ref. 14 [$E_G(H = 20\mathrm{T})$] is a coincidence, considering the important contribution of the kinetic energy to the ground-state energy. Reference 14 uses a hole mass of $m_h^* = 0.19 m_0$, while the first strong singularity in the density of states of the valence band, fitted to a single mass, results in $m_h^* = 5.1 m_0$.

[60]C. Benoît à la Guillaume, M. Voos, and F. Salvan, Phys. Rev. B 5, 3079 (1972).

[61]R. W. Martin, Solid State Commun. 19, 373 (1976).

[62]A detailed discussion of the $k$ dependence of the $e$-$p$ matrix elements appeared recently. See Ref. 30.

[63]G. Nilsson and G. Nelin, Phys. Rev. B 3, 364 (1971).

[64]Betzler *et al.* used a monochromator setup that was most sensitive to intensity variations in the center of the luminescence line, while in our setup sensitivity was flat over the total range of EHL (LA) luminescence and therefore should be more appropriate to the problem.

[65]Here $T = 0$ and $\Gamma = 0$ is assumed. Both have a negligible influence on the total intensities.

[66]A recent review on theoretical calculations is given by T. M. Rice, see Ref. 1.

[67]W. F. Brinkman and T. M. Rice, Phys. Rev. B 7, 1508 (1973).

[68]M. Combescot and P. Nozières, J. Phys. C 5, 2369 (1972).

[69]P. Vashishta, P. Bhattacharya, and K. S. Singwi, Phys. Rev. B 10, 5108 (1974).

[70]P. Bhattacharya, V. Massida, K. S. Singwi, and P. Vashishta, Phys. Rev. B 10, 5127 (1974).

[71]T. M. Rice, in *Proceedings of the 12th International Conference on Semiconductors, Stuttgart, 1974*, edited by M. H. Pilkuhn (Teubner, Stuttgart, 1974), p. 23.

[72]G. A. Thomas and Ya. E. Pokrovskii, Phys. Rev. B 18, 864 (1978).

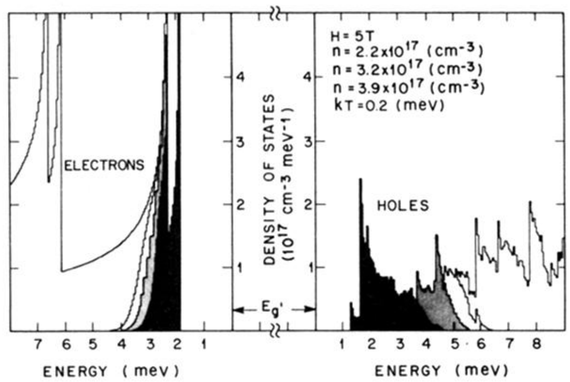


FIG. 8. Degree of population of the densities of states for conduction and valence bands at 5 T for the densities used in Fig. 7. For simplicity the total densities of states are shown.